2009

Behaviour of Reinforced Concrete Beams Retrofitted/Repaired in Shear with Fibre Reinforced Polymers

Hasan Nikopour Deilami

Behaviour of Reinforced Concrete Beams Retrofitted/Repaired in Shear with Fibre Reinforced Polymers

(SPINE TITLE: Behaviour of RC Beams Retrofitted/Repaired in Shear with FRP)
(Thesis Format: Integrated Article)

By

Hasan Nikopour Deilami

Graduate Program in Engineering Science
Department of Civil and Environmental Engineering

Submitted in partial fulfillment of the requirements for the degree of Master of Engineering Science

School of Graduate and Postgraduate Studies
The University of Western Ontario, London, Ontario
August 2009

ABSTRACT

This study aims to explore the shear behaviour of externally Fibre-Reinforced Polymer (FRP) bonded reinforced concrete beams under quasi-static or monotonic loading. The effects of key parameters such as the shear span to effective depth ratio, FRP type and scheme, and stiffness of FRP sheets on shear behaviour aspects such as the ultimate load capacity, deflection, crack pattern, mode of failure, and final strain in the FRP sheets were investigated. This study consists of two main phases incorporating experimental and numerical parts. In the experimental part, six beams were tested using different types of FRP sheets under quasi-static cyclic load and then three of these beams were repaired using epoxy injection along with new CFRP sheets and retested. A finite Element Model (FEM) was developed to predict the results of the first phase of the experimental study. The Genetic Algorithms (GAs) approach was used to develop simple, yet more accurate, formulas for predicting the ultimate load of RC beams under monotonic loading based on experimental data found in the open literature. The accuracy of the proposed model was found to be superior to that of common design guidelines namely, the ACI 440, Eurocode (EC2), Matthys model, Colotti model, and the ISIS Canada guidelines. Considerable improvement of the ultimate shear capacity of beams retrofitted using externally bonded hybrid FRP sheets was observed. The simultaneous application of epoxy injection and externally bonded FRP sheets can significantly improve the ductility and load capacity of damaged beams.

Keywords: Shear, reinforced concrete, fibre-reinforced polymers, finite element modeling, artificial intelligence.

CO-AUTHORSHIP

This thesis has been prepared in accordance with the regulation of integrated article format stipulated by the Faculty of Graduate Studies at the University of Western Ontario. Substantial parts of this thesis were submitted for publication to peer-reviewed technical journals or conferences. All experimental work, data analysis, modeling developments, and writing of the first version of publications listed below were conducted by the candidate himself. The contribution of his co-authors consisted of either providing advice, and/or helping in improving of the final version of publications:

[1] **Nikopour, H.**, Nehdi, M., Broumand, P., 2009, Experimental and Numerical Investigation of FRP Bonded-Reinforced Concrete Beams under Quasi-Static Cyclic Loading, submitted to **Canadian Journal of Civil Engineering**.

[2] **Nikopour, H.**, Nehdi, M., 2009, Shear Repair of Concrete Beams Using External FRP Sheets and Epoxy Injection Methods, submitted to **ACI Materials Journal**.

[3] **Nikopour, H.**, Nehdi, M., 2009, Modeling Shear Capacity of FRP Bonded-Reinforced Concrete Beams Using Genetic Algorithms Approach, submitted to **Journal of Materials and Structures.**

ACKNOWLEDGMENTS

I would like to express my sincere appreciation and gratitude to my thesis supervisor Prof. Moncef Nehdi for his advice and encouragement throughout all stages of my study. I also wish to thank Prof. Nehdi's research group for all the support and help during my research work.

I would like to thank Wilbert Logan for his technical advice regarding my experimental work in the Structures Lab. I would also like to thank all the administrative and technical staff in the Civil and Environmental Engineering Department for their support and cooperation.

The support of my family during my stay in Canada for this study has been most valuable.

Finally, I appreciate the support of companies which cooperated with me by providing materials or technical support including BASF, A-1 Restoration, Fibrewrap, and the Hoskin Company.

TABLE OF CONTENTS

LIST OF TABLES

LIST OF FIGURES

NOTATIONS

A_f = area of FRP external reinforcement, mm^2

A_{sl} = total area of transverse steel reinforcement, mm^2

A_{st} = total area of transverse steel reinforcement, mm^2

a = shear span of beam, mm

b = width of beam, mm

d = effective depth of beam section, mm

d_f = depth of FRP shear reinforcement, mm

d_v = $0.9d$ = effective shear depth, mm

E_c = concrete Young's modulus, MPa

E_f = tensile modulus of elasticity of FRP, MPa

E_{fl} = tensile modulus of elasticity of FRP in primary direction, MPa

E_{f2} = tensile modulus of elasticity of FRP in transverse direction, MPa

E_s = steel Young's modulus, MPa

f_{bo} = concrete biaxial compressive strength, MPa

f_{co} = concrete uniaxial compressive strength, MPa

f_c' = compressive stress in concrete, MPa

f_{fe} = effective stress in FRP, MPa

f_{fu} = design ultimate tensile strength of FRP, MPa

f_{ful} = design ultimate tensile strength of FRP in primary direction, MPa

f_{fu2} = design ultimate tensile strength of FRP in transverse direction, MPa

f_{ly} = specified yield strength of longitudinal reinforcement, MPa

f_y = specified yield strength of transverse steel, MPa

K = ratio of second stress invariant on tensile meridian to that on compressive meridian

K_1 = first modification factor for k_v

K_2 = second modification factor for k_v

L_e = active bond length of FRP, mm

n = number of plies of FRP reinforcement

R_σ = concrete stress-strain model (eq. 9) parameter usually taken as 4,

$R\varepsilon$ = concrete stress-strain model (eq. 9) parameter usually taken as 4

s = spacing of internal steel stirrups, mm

s_f = spacing of FRP shear reinforcement, mm

T_g = glass transition temperature of epoxy, °C

t_f = nominal thickness of FRP sheet, mm

V_c = nominal shear strength provided by concrete, kN

V_n = nominal shear strength, kN

V_s = nominal shear strength provided by steel, kN

V_f = nominal shear strength provided by FRP, kN

w_f = strip width of the FRP reinforcing plies, mm

α = ratio of shear span to effective shear depth

τ = nominal shear stress, MPa

τ_u = concrete-FRP bond strength, MPa

k_v = bond-dependent coefficient for shear

υ_c = Poisson's ratio of concrete

ν_{co} = effectiveness factor of concrete

υ_s = Poisson's ratio of steel

ε_0 = strain corresponding to peak compressive stress of concrete, MPa

ε_c = strain in concrete

ε_{fe} = effective FRP strain

ε_{fu} = design rupture strain of FRP

ρ = tension reinforcement ratio

ρ' = compression reinforcement ratio

ρ_f = FRP strengthening ratio

ρ_w = transversal steel reinforcement ratio

ψ = degree of shear reinforcement

ψ_e = degree of external shear reinforcement

ψ_i = degree of internal shear reinforcement

ψ_f = additional FRP strength-reduction factor

CHAPTER 1

Introduction

1.1 Background

Repairing deteriorated concrete structures for shear is essential not only to utilize them for their intended service-life, but also to assure their safety and serviceability. Several techniques have been utilized for the shear repair of RC beams such as drilling and plugging, stitching, routing and sealing, etc. More recently, the application of externally bonded FRP sheets has gained popularity compared to conventional methods. Structural strengthening with externally bonded fibre-reinforced polymers (FRP) has been recognized as a cost-effective, structurally sound and practical method for rehabilitating reinforced concrete (RC) structures (Mosallam *et al.* 2007).

The behaviour of reinforced concrete (RC) beams under shear loading is complex and difficult to predict analytically. For this reason, the shear capacity of RC beams in design codes is generally calculated using empirical or semi-empirical methods. In particular, the shear behaviour of FRP-bonded RC beams depends on the beam size, reinforcement type and amount, FRP laminate characteristics and detailing, as well as the type and position of the applied loading. In addition to the resistance of concrete, additional shear resistance contributions come from the external and/or internal reinforcements of the RC

beam. The reinforcements provided can transform the failure from brittle to ductile (Nehdi *et al.* 2007).

Several experimental and analytical studies have been carried out on RC beams retrofitted with FRP sheets having long unidirectional fibres. Currently, in the calculation of the shear capacity of FRP-bonded RC beams, design codes do not generally provide sufficient information either on various loading patterns, such as cyclic loading, or on the application of hybrid FRP sheets. Therefore, much research is needed to explore the behaviour of RC beams retrofitted with hybrid FRP sheets. In particular, their ultimate strength, pattern of failure and performance under cyclic loading need to be understood to pave the way for their full-scale use in construction.

1.2 Objectives of study

The main objectives of this study are to:

1) Develop experimental data on the ultimate shear load capacity, deflection, crack pattern, mode of failure, and strain in FRP sheets for reinforced concrete beams retrofitted using hybrid FRP sheets as external reinforcement under quasi-static cyclic loading.
2) Experimentally investigate the effect of repairing cracks using epoxy injection for damaged reinforced concrete beams retrofitted using FRP sheets, under shear loading.

3) Investigate the effects of main parameters that affect the shear behaviour of reinforced concrete beams retrofitted by FRP sheets, such as the shear span to depth ratio *a/d*, longitudinal reinforcement ρ, and the mechanical and geometrical characteristics of the attached FRP sheets.
4) Using the Genetic Algorithm's approach for the prediction of the shear capacity of reinforced concrete beams retrofitted by FRP sheets.

1.3 Scope of Research

This thesis consists of five chapters. Chapter 1 provides an introduction on using FRP sheets as external reinforcement in concrete structures, presents the objectives of the study, and summarizes the layout of the thesis. Chapter 2 analyses previous work in the open literature, with particular focus on existing research developing numerical equations or experimental databases on retrofitting or repairing concrete beams using externally bonded FRP sheets or epoxy injection. Chapter 3 describes in detail the experimental program on reinforced concrete beams retrofitted by FRP sheets along with finite element method to model the results of experimental work. Chapter 4 describes experimental work on repairing damaged RC beams using epoxy injection and FRP sheets and testing them under monotonic loading. Chapter 5 presents a numerical study on the effects of different parameters such as the shear span to depth ratio *a/d*, longitudinal reinforcement ρ, mechanical and geometrical characteristics of attached FRP sheets using artificial intelligence namely Genetic Algorithms approaches. Chapter 6 presents the conclusions reached in this study along with some recommendations for future research.

CHAPTER 2

Overview of Previous Work on Application of Externally Bonded FRP Sheets and Epoxy Injection for Rehabilitation

Historically, concrete members have been repaired by post-tensioning or jacketing with new concrete in conjunction with surface adhesives (Klaiber *et al.* 1987). Since the mid 1960's, epoxy bonded steel plates have been used in Europe and South Africa to retrofit flexural members (Dussek 1987). Steel plates have a durability problem unique to this application, because corrosion may occur along the adhesive interface. This type of corrosion adversely affects the bond at the steel plates/concrete interface and is difficult to monitor during routine inspections. Additionally, special equipment is necessary to install the heavy plates. As a result of these problems, alternative materials have been sought by engineers.

2.1 External FRP for Rehabilitation of Concrete Beams

There is a large need for strengthening and retrofitting concrete structures all over the world. The reasons for such a need include, increased load demand, design and construction faults, problems initiated by temporary overload, and so on. Some structures are in such a bad condition that they need to be replaced. Since environmental and economic factors preclude replacing all such structures, they should instead be strengthened or retrofitted as much as possible. A repair and strengthening method that

has gained acceptance all over the world is plate bonding with fibre-reinforced polymers (FRPs), (Burgoyne 1999; Labossière 2000; Bencardino *et al.* 2002; Shin and Lee 2003). This method, which has now been used for over a decade, consists of a thin layer of fibre composite epoxy bonded externally to a structure's surface so that the composite acts as an outer reinforcement.

2.1.1 *Fibre reinforced polymers (FRP)*

FRPs are used in the aerospace and automotive fields because of their high strength to weight ratio, durability, and ability to form complex shapes. They are generally constructed of high performance fibres such as carbon, Aramid, or glass which are placed in a resin matrix. By selecting among the many available fibres, geometries and polymers, the mechanical and durability properties can be tailored for a particular application. This quality makes FRP a good choice for civil engineering applications.

Carbon fibres have a high elastic modulus and high strength in both tension and compression. Composed almost entirely of carbon atoms, the fibres are generally available as bundles of 500-150,000 filaments of approximately five microns in diameter called "yarn". These are then assembled directly into FRP products or into intermediate forms such as continuous fibre sheets or fabrics. Continuous fibre sheets are made of parallel yarns attached to flexible backing tape for handling. Fabrics are made of yarns stitched into a geometric form. The yarns may run unidirectionally like continuous fibre sheets, or be woven at different angles into a fabric. Carbon fibre-reinforced polymers

(CFRPs) have a high strength and stiffness-to-weight ratio, show excellent fatigue Behaviour and corrosion resistance, and are not magnetic. The structure of carbon fibres is represented schematically in Fig. 2.1. Table 3.1 shows mechanical properties of typical fibres. As illustrated in Table 3.1 carbon fibres are highly anisotropic and have different strength and stiffness in the axial and radial directions.

Most glass fibres are based on silica (SiO_2), with additions of oxides of calcium, born, sodium, iron and aluminum. These glasses are usually amorphous, although some crystallization may occur after prolonged heating at high temperature, leading to a reduction in strength. There are three types of glass fibres. The most commonly used glass fibre, E-glass (E for electrical), draws well and has good strength, stiffness, electrical and weathering properties, In some cases, C-Glass (C for corrosion) is preferred, having a better resistance to corrosion than E-glass, but a lower strength. Finally S-glass (S for strength) is more costly than E-glass, but has a higher strength, Young's modulus and temperature resistance. The diameter of E-glass fibre is usually between 8 and 15 μm. An example is given in Fig. 2.2 of a section cut normal to the fibre direction in a lamina with high glass fibre content.

Aramid is one of the most common organic fibres. It was first developed by Du Pont with the trade name Kevlar. The principles involved are best understood by considering fibres based on a simple polymer, polyethylene. Chain-extended polyethylene single crystals consist of straight zig-zag carbon backbone chains, fully aligned and closely packed. These have a Young's modulus of about 220 GPa parallel to the chain axis. Fairly good

chain alignment can be achieved in a fibre by drawing and stretching resulting in a modulus of 70 GPa. As for carbon fibres, the modulus normal to the fibre axis is much less than that along the fibre axis.

Since there is usually no adhesion between individual fibres, a polymer resin matrix is used to transmit forces between the fibres. Polymers, such as epoxy have the advantages of lower cost, ease of workability, and somé have good resistance to environmental effects. The hand or contact layup is the oldest method of assembling an FRP. The epoxy is applied to one or both sides of the fabric and worked between the fibres using an ordinary paint roller and hand pressure. The surface may then be finished with a flexible blade to remove excess epoxy before curing occurs. Fibres may be mixed in random directions with suitable epoxy or they may be arranged in specific directions (Fig. 2.3). Another method for the arrangement of fibres is the woven structure, which is shown in Fig. 2.4.

The most commonly used test method for determining the properties of a composite material is the uniaxial tension test (ASTM D3552 -96, 2007). In this test, a specimen of FRP is instrumented either using an extensiometer or strain gages and is loaded in tension. The elastic modulus varies for different fibre orientations. When the load is applied at 0^{o} or 90^{o} to the fibres, the behaviour is almost linear elastic. However, when the load is applied at an angle to the fibres, the behaviour is nonlinear.

2.1.2 *Shear retrofit of RC beam using FRP*

Several experimental researches have been carried out on the investigation of the shear retrofit of damaged or low strength reinforced concrete RC beams using externally bonded FRP sheets under monotonic loading. They have used different schemes and materials. The most typical schemes are two side, three sides bonded or completely wrapped patterns. Some of the experimental work includes researches by Mosallam *et al.* 2007, Khalifa *et al.*1999, Cao *et al.* 2005, Abdel-Jaber *et al.* 2003, Kachlakev *et al.* 1999, Kage *et al.* 1997, Mitsui *et al.* 1998, Sato *et al.* 1996, Triantafillou 1998, Uji 1992, Huthchinson *et al.* 1999, Taerwe *et al.* 1997, Taljsten *et al.* 1999, Michael *et al.* 1995, Carolin *et al.* 2005, Pellegrino *et al.* 2006, Hadi 2003, Monti *et al.* 2006, Matthys 2000, Spadea *et al.* 1998, Swamy *et al.* 1996, Norris *et al.* 1997, Umezu *et al.* 1997, Araki *et al.* 1997, Swamy *et al.* 1999, Chajes *et al.* 1995, Al-Sulaimani *et al.* 1994. Their results show completely wrapped schemes provide better results for shear retrofitting of RC beams compared to other schemes. Moreover it was concluded even though external FRP increase ultimate shear capacity, it may decrease ductility in some circumstances. Failure of the beam can be cause by debonding or rupture of FRP sheets or failure mode may turn to a flexural one.

2.1.3 *Current shear design guidelines for FRP-RC beams*

Some analytical and empirical models have been developed to theoretically predict the shear capacity of externally bonded FRP reinforced concrete beam specimens, and are described below.

ACI 440, CSA 860, ISIS Canada models

The model proposed by ACI 440 (2003) is applicable to reinforced concrete beams with externally applied FRP reinforcement. According to this model, the nominal shear strength V_u of such beams is given by

$$V_n = V_c + V_s + \psi_f V_f \tag{2.1}$$

Where V_c is the nominal shear capacity provided by concrete, V_s is the nominal shear capacity provided by steel, V_f is nominal shear capacity provided by the fibre-reinforced polymer sheet, and ψ_f is the additional reduction factor given in Table 10.1 of the ACI 440 document.

The shear strength contribution from the FRP is:

$$V_f = \frac{A_f E_f \varepsilon_{fe} d_f}{s_f} \tag{2.2}$$

and

$$V_c = \left(0.16\sqrt{f_c'} + 17\frac{\rho_l V_u d}{M_u} \right) bd \tag{2.3}$$

$$V_s = \frac{A_{st} f_{ty} d}{s} \tag{2.4}$$

In the above formulas, d is the effective depth of the beam section, $M_u / V_u d$ represents the shear span to depth ratio a/d, and $d_f = h_f - d'$ is the effective depth of the external reinforcement, d' being the concrete cover. Furthermore, ε_{fe} is the effective tensile strain in the FRP and E_f is the elastic modulus of the FRP in the principal fibre orientation.

The effective strain, ε_{fe} in the FRP is assumed to be smaller than the ultimate strain, ε_{fu}. This can be computed as

$$\varepsilon_{fe} = \begin{cases} 0.004 \le 0{,}75\varepsilon_{fu} & \text{completely wrapped beams} \\ k_v \varepsilon_{fu} \le 0.004 & \text{two or three sides laminated} \end{cases} \tag{2.5}$$

$$k_v = \frac{k_1 k_2 L_e}{11{,}900\varepsilon_{fu}} \le 0.75 \tag{2.6}$$

$$L_e = \frac{23{,}300}{(nt_f E_f)^{0.58}} \tag{2.7}$$

$$k_1 = \left(\frac{f_c'}{27}\right)^{2/3} \tag{2.8}$$

$$k_2 = \begin{cases} \dfrac{d_f - L_e}{d_f} & \text{U - wraps} \\ \dfrac{d_f - 2L_e}{d_f} & \text{two sides laminated} \end{cases} \tag{2.9}$$

Where, f_c' and E_f are in MPa, and t_f in mm, respectively. The Canadian Standards Association CSA S806 (2002) and ISIS Canada (2001) design manuals use similar methodology to the ACI code. Figure 2.5 illustrates parameters used in the ISIS approach.

Triantafillou and Antonopoulos model

This model proposed by Triantafillou and Antonopoulos (2000) has been adopted by the Eurocode (EC2). According to this model

$$V_n = V_c + V_s + V_f \le V_{R2} = 0.4 v_{co} f_c' \, bd \tag{2.10}$$

Where

$$V_c = \tau_R k(1.2 + 40\rho_l)bd \tag{2.11}$$

$$V_s = \frac{0.9A_{st}f_{ty}d}{s} \tag{2.12}$$

$$V_f = \frac{0.9A_f E_f \varepsilon_{fe} d_f}{s_f} \tag{2.13}$$

The tensile strength of concrete, $f_{ct} = 0.3(f_c')^{2/3}$, the concrete shear resistance, $\tau_R = 0.025 f_{ct}$, k=1.6-d >1 (d is in m), $\rho_l = \frac{A_{sl}}{bd}$, $\rho_f = \frac{A_f}{bs_f}$, and $\nu_{co} = 0.7 - f_c'/200 \geq 0.5$ (f_c' is in MPa).

The effective strain in this model is:

$$\varepsilon_{fe} = \begin{cases} 0.17\left(\frac{f_c^{2/3}}{E_f\rho_f}\right)^{0.30}\varepsilon_{fu}, \text{ for beams fully wrapped with CFRP} \\ min\left[0.00065\left(\frac{f_c^{\frac{2}{3}}}{E_f\rho_f}\right)^{0.56}; 0.17\left(\frac{f_c^{\frac{2}{3}}}{E_f\rho_f}\right)^{0.3}\varepsilon_{fu}, \text{ for two or three sides laminated with CFRP}\right] \end{cases} \tag{2.14}$$

Matthys and Triantafillou model

Matthys and Triantafillou (2001) made a modification to the Trinatafillou and Antonopoulos model and incorporated the effect of the shear span to beam depth ratio in the calculation of the effective strain. In practice, it was proposed to calibrate the

effective FRP strain, ε_{fe} not only in terms of the FRP axial rigidity, $E_f \times \rho_F$ and the concrete tensile strength, f_{ct}, but also taking into account the influence of the shear span ratio *a/d*. According to their modification, the effective strain can be expressed as:

$$\varepsilon_{fe} = \begin{cases} 0.72\varepsilon_{fu} e^{-0.0431\Gamma_f} & \text{fully wrapped wit CFRP} \\ 0.56\varepsilon_{fu} e^{-0.0455\Gamma_f} & \text{two or three sides laminated CFRP} \end{cases} \quad (2.15)$$

Where

$$\Gamma_f = \frac{E_f \rho_f}{f_c^{\frac{2}{3}} \left(\frac{a}{d}\right)} \quad (2.16)$$

The remaining expressions for the evaluation of the ultimate shear capacity V_u in this model are the same used in the Triantafillou and Antonopoulos model, expressed in equations 2.12, 2.13 and 2.14.

Colotti *et al.* model

Colotti *et al.* (2004) proposed that the total contribution to shear reinforcement can be expressed as:

$$\psi = \psi_i + \psi_e \quad (2.17)$$

The internal shear strength contributed by the internal steel reinforcement is:

$$\psi_i = \frac{A_{st} f_y}{b s f_c'} \tag{2.18}$$

whereas, the external contribution from FRP is:

$$\psi_e = \begin{cases} \dfrac{2w_f t_f}{b s_f f_c'} f_{fe} & \text{for completely wrapped beams} \\ min\left(\dfrac{w_f d_f}{b s_f f_c'} \tau_u ; \dfrac{2w_f t_f}{b s_f f_c'} \right) & \text{two or three sides laminated} \end{cases} \tag{2.19}$$

where the effective stress, $f_{fe} = v_f \times f_{fu}$.

The shear strength of a beam specimen is given by:

$$V = (\frac{\tau}{f_c'}) b d_v f_c' \tag{2.20}$$

where τ / f_c' is the minimum value from the following failure cases:

Failure case (1)

$$\frac{\tau}{f_c'} = \begin{cases} \dfrac{1}{2}\left[\sqrt{1+\alpha^2} - \alpha\right] + \psi\alpha & 0 \le \psi \le \psi_0 = \dfrac{\sqrt{1+\alpha^2} - \alpha}{2\sqrt{1+\alpha^2}} \\ \sqrt{\psi(1+\psi)} & \psi_0 \le \psi \le 0.5 \\ \dfrac{1}{2} & \psi > 0.5 \end{cases} \tag{2.21}$$

Failure case (2)

For $\psi \le \psi_0$

$$\frac{\tau}{f_c'} = \begin{cases} \frac{1}{2}\left[\sqrt{4\eta(1-\eta)+\alpha^2} - \alpha\right] & \eta \le 0.5 \\ \frac{1}{2}\left[\sqrt{1+\alpha^2} - \alpha\right] & \eta > 0.5 \end{cases} \tag{2.22}$$

For $\psi > \psi_0$

$$\frac{\tau}{f_c'} = \psi\left[\sqrt{\frac{2\eta}{\psi}+\alpha^2} - \alpha\right] \tag{2.23}$$

where $\eta = \frac{A_{sl} f_{ly}}{b d_v f_c'}$ and $\alpha = \frac{a}{d_v}$.

The effectiveness of this design procedure can be assured by predicting the internal strengths corresponding to the different failure modes of the member. Thus, it is possible to select the geometry and mechanical properties of the composite material to ensure fewer unfavourable failure modes.

All design guidelines presented in this chapter do not consider the interaction between the internal shear reinforcement and the shear capacity owing to the FRP. Also, design provisions are not applicable for hybrid or bidirectional FRP sheets. Except the Matthys and Triantafillou model, other formulas do not consider the effect of the shear span-to-depth ratio on the shear capacity contributed by the FRP. Mosallam *et al.* (2007) argued that shear span-to-depth ratio *a/d*, is an important factor that actively controls the shear failure mode of beam and consequently influences the shear strength enhancement. Pellegrino (2006) showed that there is a considerable interaction between steel stirrups and external FRP laminates and that it is possible at failure, weather in-debonding or

rupture, stress level in steel stirrups are much lower than the yield stress. Sakar *et al.* (2009) presented an experimental research on RC beams with bidirectional FRP sheets as external reinforcement. He concluded that current design codes have a substantial error due of ignoring the FRP effect in the transverse direction.

2.2 Repairing of Cracks in Damaged RC Beams

Concrete is one of the most versatile construction materials and the most consumed material worldwide after water. It is relatively inexpensive, durable, strong, and it can be molded into any shape. The development of concrete as a construction material dates back to several thousand years, while steel was introduced to reinforce concrete about two centuries ago. There have been tremendous advancements in the use of reinforced concrete for construction over the last decades (Shah, 2005).

Although the majority of concrete structures have generally performed satisfactory, many problems have been reported due to one or more of the following causes: (i) improper quality of materials, (ii) incorrect specifications, (iii) faulty design, (iv) errors in the construction process, and (v) exposure of structures to extreme environmental conditions. All of these problems may lead to insufficient structural capacity and/or the development of cracks which can decrease the service life of structures. A successful repair technique improves the performance of a structure, restores and/or increases its strength and stiffness, enhances the appearance of the concrete surface, prevents the ingress of

moisture, chloride ions and carbon dioxide to the reinforcing steel, and improves the overall durability.

Cracks can be categorized into three groups: (i) cracks due to inadequate structural performance, (ii) cracks due to inadequate material performance, and (iii) acceptable cracks. Structural cracks are caused primarily by overloading; material related cracks are due to shrinkage and chemical reactions; and acceptable cracks are those that develop due to service loading for tensile stresses to be distributed properly along the length of the material (Tsisatas *et al.* 1994). Cracks in structural elements can also be classified as dormant or active. Active cracks, such as cracks caused by foundation settlement, cannot generally be fully repaired, whereas dormant cracks can be successfully repaired (Ekenel *et al.* 2007).

Various systems for crack repair have been developed and used for many years. The most common crack repair materials are cementitious and polymer products and include epoxy injection and grouting. The ACI Publication 546R-96 (1996) "Concrete Repair Guide" documents standard techniques for concrete repair with cementitious and polymer materials. Two other ACI publications, which are directly related to crack repair, include 224R-80 "Control of Cracking in Concrete Structures" (1980), and ACI 224.1R-93 "Cause, Evaluation, and Repair of Cracks in Concrete Structures" (1993). According to ACI 224.1R-93, any crack repair material and method must not only address the cause of the cracking, but also repair the crack itself. Epoxy resins are commonly used repair materials that generally have very good bonding and durability characteristics. In the

following sections the most common methods for repairing cracks have been briefly discussed.

2.2.1 *Conventional methods for repairing cracks*

Three common methods for repairing cracks in concrete structures are as follows:

- Routing and sealing
- Stitching
- Drilling and plugging

Routing and sealing

Figure 2.6 illustrates different steps of this method. It involves enlarging the crack along its exposed face and filling and sealing it with a suitable joint sealant. It is a useful technique for horizontal surfaces such as floors and pavements owing to as ease of application. Materials which are usually used for this approach are epoxies, urethanes, silicones, polysulfides, asphaltic materials, and polymer mortars (Johnson, 1965). The procedure consists of:

1-Preparing a groove at the surface

2-Cleaning by air blasting or water blasting followed by drying

3-Sealant is placed into the dry groove and allowed to cure

Stitching

The most common stitching methods use stitching dogs (U-shaped metal units), thin metal interlocking plates, or dowel bars for reinforcement. In each method, the reinforcement is installed across the crack and is bonded to each side of the crack with epoxy or cementitious materials. The amount of reinforcement can be varied to achieve the desired strength restoration. Unlike interlocking plates and dowel bars, which are embedded in the concrete, stitching dogs are surface mounted. Since concrete is usually weak in axial tension, stitching dogs are placed on both faces. Stitching dogs are most effective when restoring tension in bending members since they are placed at the critical location-the tension face.

To install stitching dogs, holes are drilled on both sides of the crack, the holes are cleaned, and the legs of the dog are anchored in the holes with non-shrink grout or epoxy. The length, orientation, and location of the stitching dogs are varied so that the tension is transmitted across the area, not across a single plane within the section.

Because dogs are thin and long and are not supported laterally, they cannot take much compressive force. If the crack closes as well as opens, the dogs must be stiffened and strengthened to prevent buckling. One method to prevent buckling is to embed the dogs in an overlay.

Dowel bars are also used to repair concrete cracks. To install dowel bars, two holes are drilled diagonally through the crack, one from each side. The holes are filled with non-shrink cementitious or epoxy materials, then a dowel bar is driven into each hole. The bonded dowel bars transmit force across the crack face. The angled dowel bars restore shear transfer and transmit axial tension, but are not very effective for restoring tension in flexural members. (Contrasto, 1995). Figure 2.7 presents an example of using this method.

Drilling and plugging

This method consists of drilling down the length of the crack and grouting it to form a key. It is most often used to repair vertical cracks in retaining walls.

2.2.2 *Epxoy injection*

One way to repair extensive cracks is the use of epoxy injection. This technology was developed in Germany and Switzerland in the 1930's. It can be used to restore tensile strength to a cracked concrete member such as slabs and pavements, beams, walls and columns. Usually a two component epoxy is used in this method, one of which is a resin and the other is a hardener material. Figure 2.8 shows crack repair using epoxy injection. The typical installation procedure is as follows:

- Prepare the surface
- Seal cracks and install injection ports

- Inject the resin
- Cure
- Grind off seal and ports

The common installation problems associated with the epoxy injection can be summarized as follows:

- Improper resin
- Improper mixing
- Inadequate surface sealing
- Improper pressure
- Improper port spacing
- Improper sequence of pumping
- Excessive crack width

Calder and Thompson (1998) reported that the overall structural performance of RC slabs repaired using epoxy resin injection performed best compared to other repair materials such as polyester and methyl methacrylate resins. The stiffness of the cracked slabs in their study was about one quarter of that of the un-cracked slabs and the repairs reinstated only about half of the stiffness loss. According to Minoru *et al.* (2001), the bond between concrete and the injection material is very critical; a good bond may restore the original stiffness of the repaired material and prevent further penetration of chloride ions and water. The crack should also be clean and dry prior to injection. Epoxy injection is not

applicable if the cracks are actively leaking or cannot be dried out, unless moisture tolerant epoxies are used which can flush the moisture from the inner crack surfaces.

2.3 Conclusions and Motivation of the Research

A literature review was carried out to critically examine the research available on using externally FRP bonded and epoxy injection as renovation and upgrading methods for RC beams. It was argued that FRP sheets have a great potential for retrofitting concrete structures. The main advantage of FRP sheets is their ability to mitigate corrosion problems while having a high strength-to-weight ratio. Research on the application of externally bonded unidirectional FRP sheets for reinforced concrete (RC) beams under monotonic loading is well established. However, very limited research on the shear behaviour of externally FRP-bonded reinforced concrete beams is available using hybrid FRP sheets or under other types of loading such as cyclic loading. Some design provisions were discussed in this chapter, but they do not consider the interaction between the internal shear reinforcement and the shear capacity imparted by the FRP. Moreover, design codes are not applicable for hybrid or bidirectional applications of FRP sheets. The effect of the shear span-to-depth ratio a/d is also ignored in all models, expect the Matthys and Triantafillou model. Thus, more research is still needed to improve the accuracy of design provisions and to develop a data-base on other patterns of loading and FRP materials.

Three conventional methods for repairing cracks were discussed. Epoxy injection was found to be a powerful and simple method for repairing damaged concrete structural members. However, data on the simultaneous application of epoxy injection and externally bonded FRP sheets is scarce.

Table 2.1: Typical fibre properties

Fibre	Density, P ($Mg\ m^{-3}$)	Young's modulus E (GPa)	Poisson's Ratio ν	Tensile strength σ (GPa)	Failure strain ε (%)	Thermal expansivity α ($10^{-6}K^{-1}$)	Thermal conductivity α ($W\ m^{-1}\ K^{-1}$)
HM[a] Carbon	1.95	axial 380 radial 12	0.2	2.4	0.6	axial -0.7 radial 10	axial 105
HS[b] Carbon	1.75	axial 230 radial 20	0.2	3.4	1.1	axial -0.4 radial 10	axial 24
E-glass	2.56	76	0.22	2.0	2.6	4.9	13
Kevlar	1.45	axial 130 radial 10	0.35	3.0	2.3	axial -6 radial 54	axial 0.04

[a] High modulus
[b] High strength

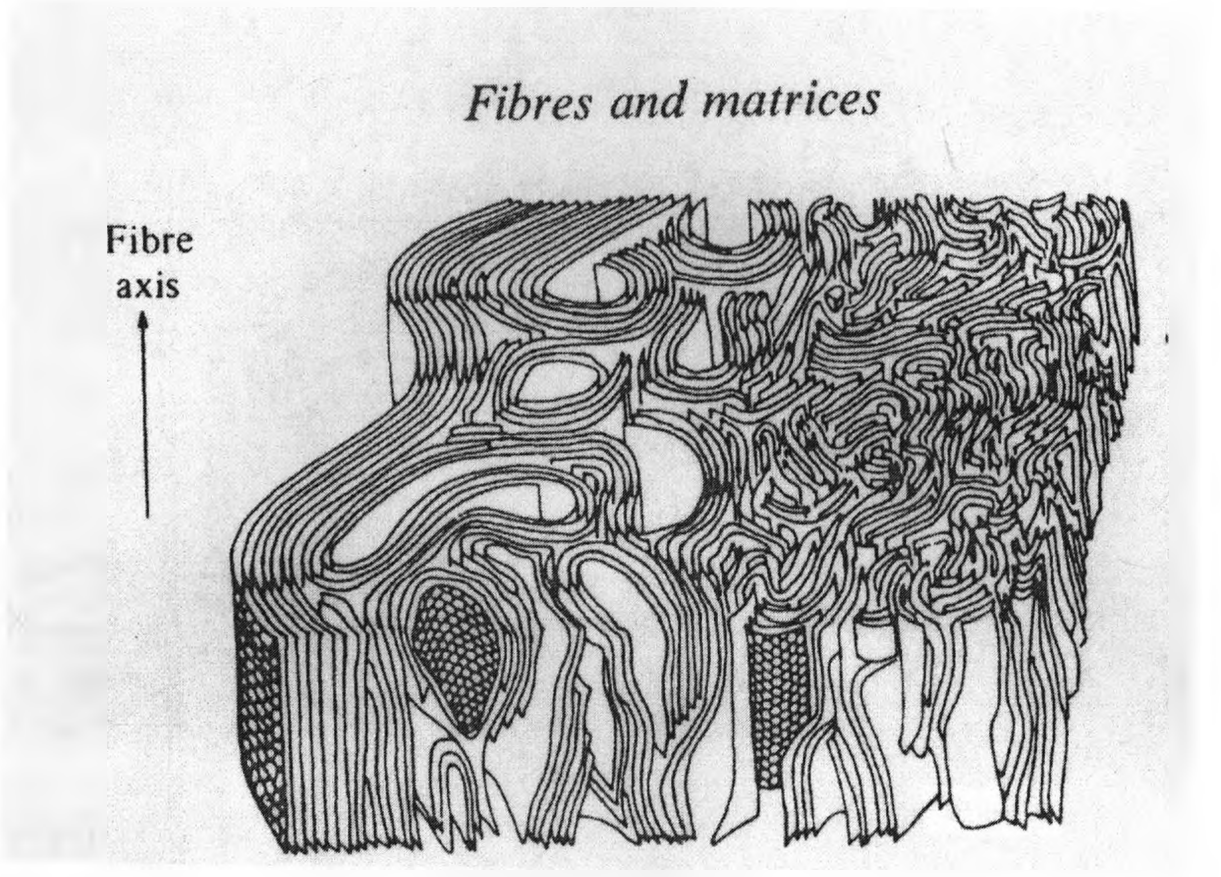

Fig. 2.1: Schematic representation of the structure of carbon fibres (From Bennett and Johnson, 1978).

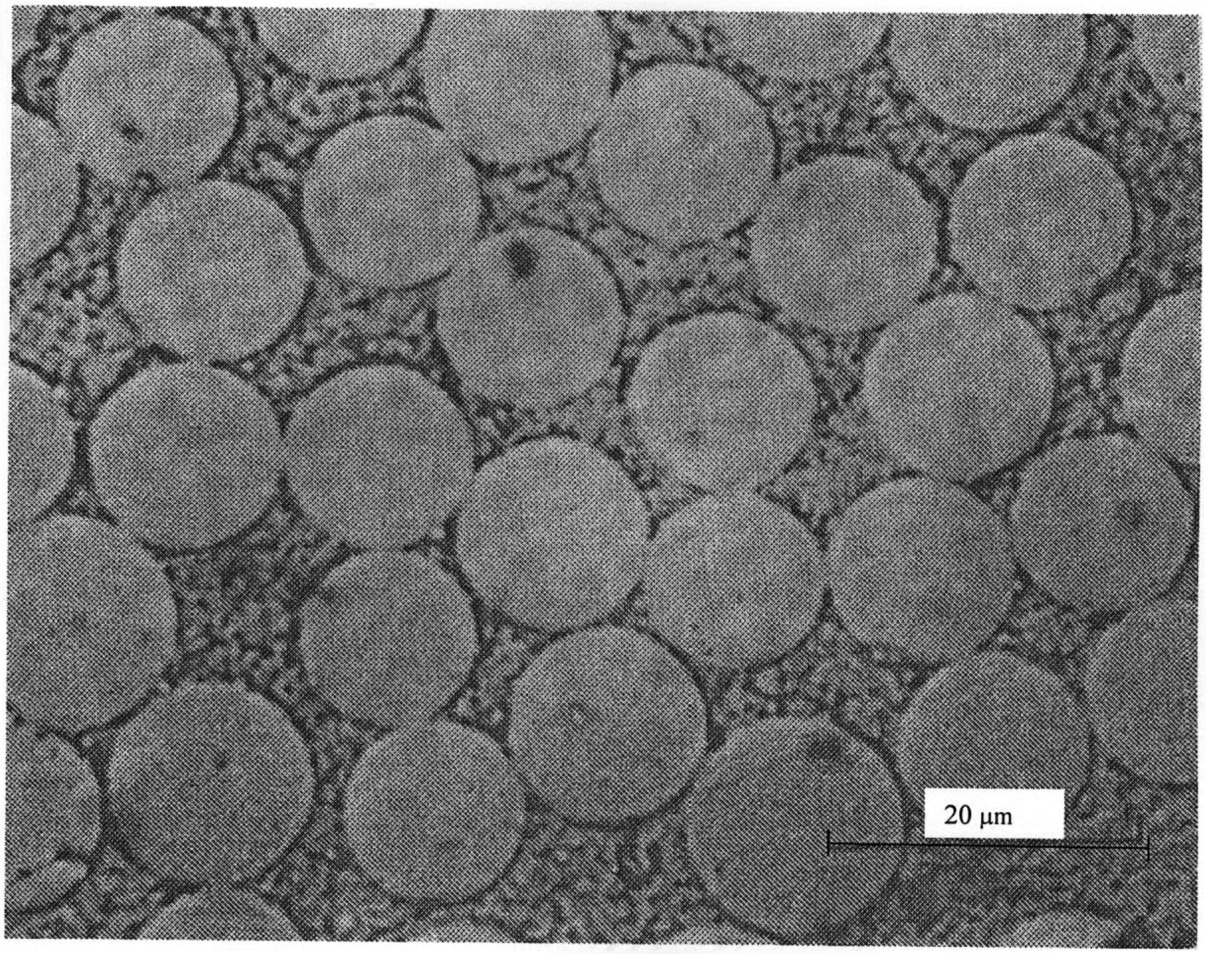

Fig. 2.2: Optical micrograph of a section cut at right angles to fibres in a unidirectional laminate of glass fibre/polyester resin (From Hull and Clyne, 1996).

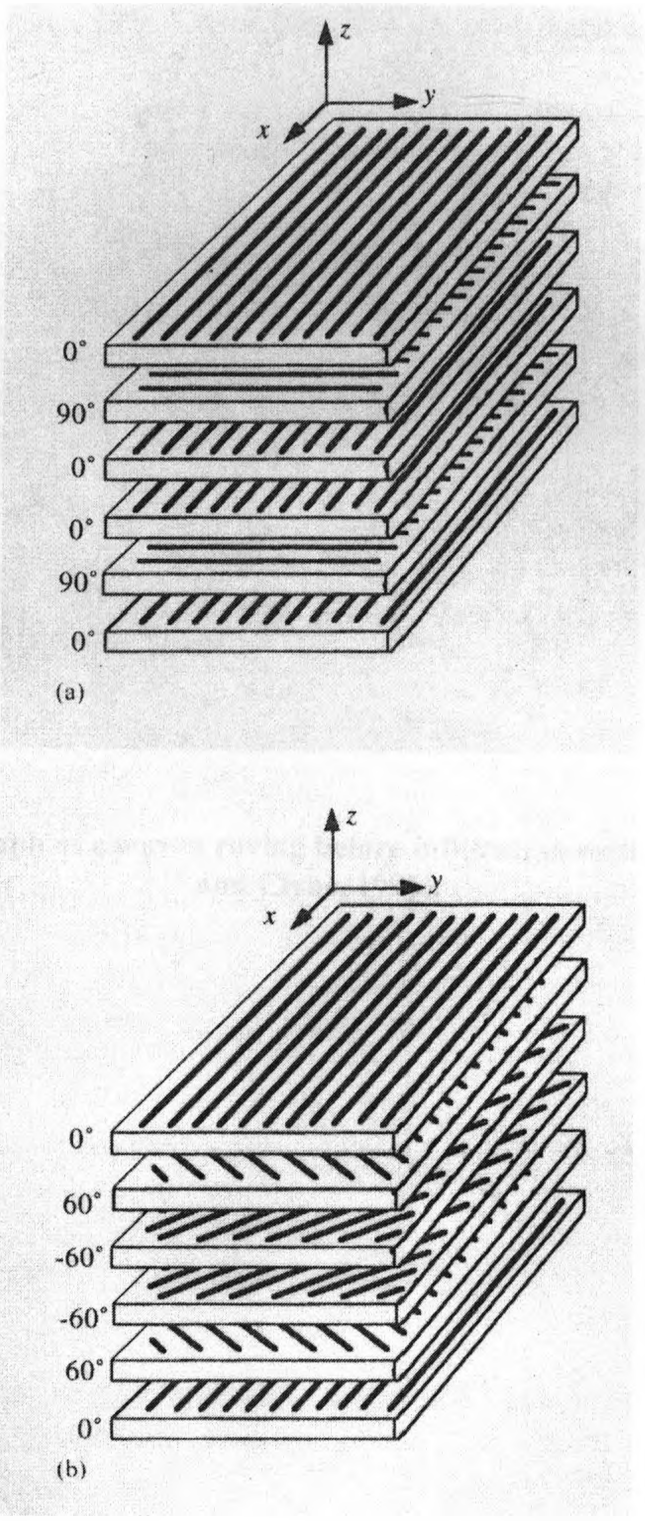

Fig. 2.3: Arrangement of plies in (a) a crossply laminate, and (b) an angle-ply laminate sandwiched between 0^0 plies (From Hull and Clyne, 1996).

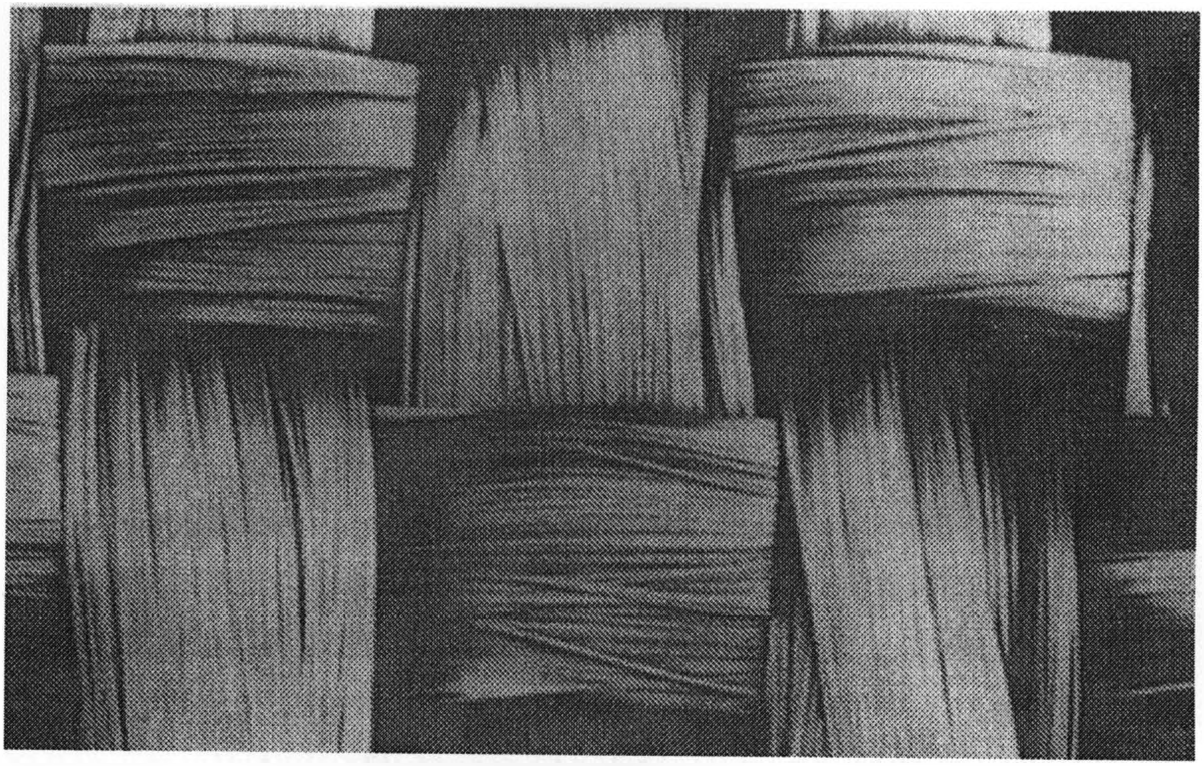

Fig. 2.4: Micrograph of a woven roving before infiltration with resin (From Hull and Clyne, 1996).

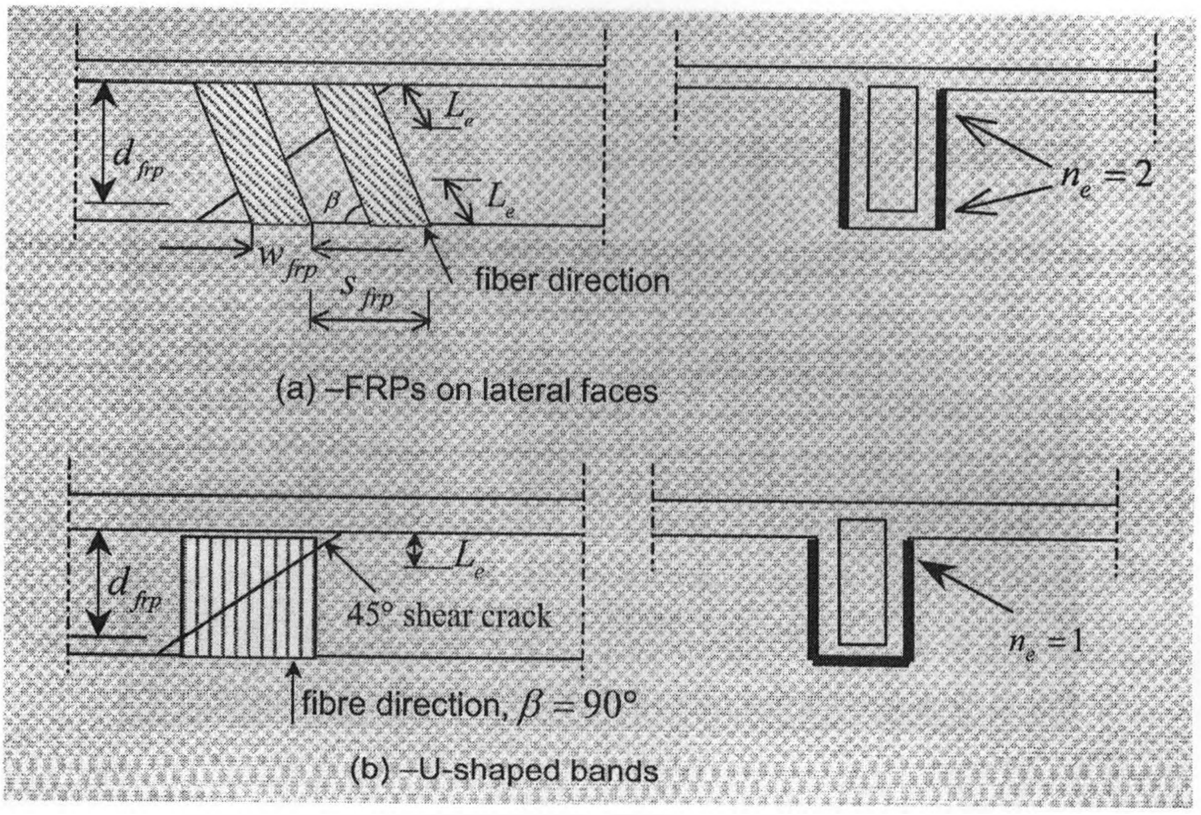

Fig. 2.5: Typical shear strengthening and design parameters (From ISIS Canada Design Manual No.2, 2001).

Fig. 2.6: Repair of crack in pavement by routing and sealing (From *http://www.highwayimprovementinc.com/crack_sealing.htm*).

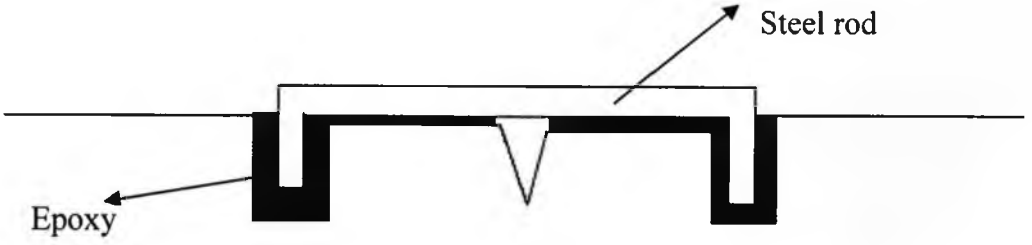

Fig. 2.7: Stitching method for repairing cracks.

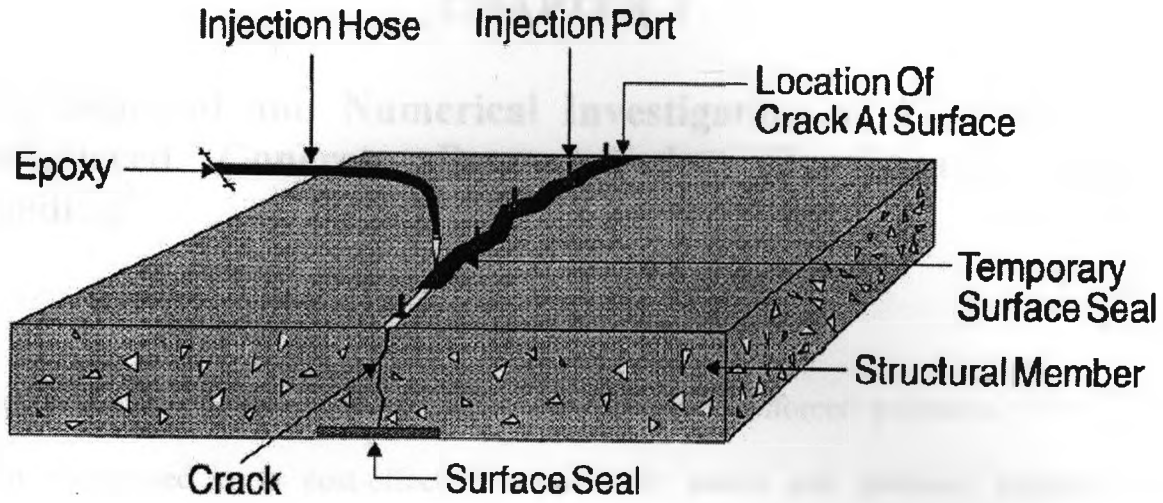

Fig. 2.8: Crack repair using epoxy injection (From Sika Tech Guide, 1990).

CHAPTER 3

Experimental and Numerical Investigation of FRP Bonded-Reinforced Concrete Beams under Quasi-Static Cyclic Loading[1]

Structural strengthening with externally bonded fibre-reinforced polymers (FRP) has been recognized as a cost-effective, structurally sound and practical method for rehabilitating reinforced concrete (RC) structures. Although several experimental and numerical studies have been carried out on the shear capacity of RC beams retrofitted by carbon or glass fibre-reinforced polymers, there has been little work on hybrid FRP sheet applications, particularly under cyclic loading. In the present research, six RC beams were constructed, and four of which were retrofitted using various schemes of FRP sheets. All beams were subjected to quasi-static cyclic loading in an attempt to represent the effect of fatigue and repetitive loading. The experimental crack load, ultimate load, and deflection pattern at mid-span of the beams were measured and compared with predictions of a numerical model based on finite element analysis. Experimental results demonstrated that hybrid applications of FRP sheets can improve the shear performance of retrofitted RC beams and increase the ultimate strain of the FRP sheets at failure. The results of the numerical model were in reasonable agreement with the corresponding experimental results.

[1] A version of this chapter has been submitted for review to a Canadian Journal of Civil Engineering.

3.1 Introduction

Innovative composite materials known as fibre-reinforced polymers (FRP) have shown great promise in the rehabilitation of ageing reinforced concrete (RC) structures. The rehabilitation of these structures is usually in the form of strengthening of structural members, repair of damaged structures, or retrofitting for seismic deficiencies. Composite materials have proven to be an excellent option for external reinforcement because of their high tensile strength, lightweight, resistance to corrosion, high durability, and ease of installation (Khalifa et al. 2000). Externally bonded FRP reinforcement has shown to be applicable to the strengthening of many types of RC structures and structural members such as columns, beams, slabs, walls, tunnels, chimneys, and silos. It can be used to improve the flexural and shear capacities, and also to provide confinement and ductility of structural members, particularly under compressive load (Khalifa et al. 2000).

The shear behaviour of FRP-bonded RC beams depends on a number of parameters including the beam size, reinforcement type and amount, FRP laminate properties and detailing, and the type of the applied loading (Pellegrino et al. 2006). Several studies have been done on the application of unidirectional fibres for retrofitting reinforced concrete beams; however, very little information is available of behaviour of beams retrofitted by hybrid FRP sheets.

Over the past few years, a number of experimental and theoretical studies have been carried out on the behaviour of hybrid FRP sheets used as external reinforcement for RC

structures. For instance, Wu et al. (2008) carried out an experimental research on the application of hybrid FRP sheets as external confinement for concrete cylinders. They concluded that this reinforcement scheme can significantly enhance the strength and ductility, resulting in a large energy absorption capacity of specimens. Li et al. (2002) conducted an experimental study on the reinforcement of concrete beam–column connections with hybrid FRP sheets. Their results show that retrofitting critical sections of concrete frames with FRP reinforcement can provide significant gains in strengthening and stiffening of such frames and improving their behaviour under different types of loading. The selection of the type of FRP and its architecture in order to improve the bond and strength of the retrofitting scheme were also discussed in this study. Li et al. (2005) later reported the results of an experimental study conducted on RC beams retrofitted in flexure using hybrid FRP sheets. It was indicated that hybrid sheets allow the transfer of stress in the hybrid composite between carbon fibres and glass fibres, and further improve ductility. Based on this experimental study, an elastoplastic section analysis method was conducted to predict the bearing capacity of RC beams strengthened with hybrid FRP sheets. Sakar et al. (2009) reported results of an experimental research on the application of bidirectional CFRP sheets for retrofitting RC beams under cyclic loading. It was concluded that adding a horizontal ply in the 0^{o} direction has a considerable effect of increasing the shear capacity.

No research was accessible in the open literature on the application of hybrid sheets of different FRP materials as external reinforcement for the shear rehabilitation of RC beams. To develop experimental data on the ultimate shear load capacity, deflection,

crack pattern, mode of failure, and strain for RC beams retrofitted using hybrid FRP sheets as external reinforcement under quasi-static cyclic loading, six full-scale beams were constructed and tested in this study. One beam specimen was retrofitted using hybrid sheets of carbon fibres in the main direction and Aramid fibres in the transverse direction. The same scheme was implemented using carbon and glass fibres on another RC beam specimen. To compare the results with that for RC beams with normal unidirectional FRP fibres, one beam specimen was retrofitted using unidirectional carbon fibre sheets as external reinforcement. Another beam specimen had woven glass fibres in the both $+45^{\circ}/-45^{\circ}$ diagonal directions. The last two RC beams tested had no external reinforcement.

All beams were loaded using an eight point loading scheme. Strain gauges were installed at three directions on the surface of the four RC beam specimens with varying external FRP types and schemes. All beam specimens were loaded to failure under quasi-static cyclic loading. To relate experimental results to theory, the finite-element technique was utilized.

3.2 Experimental Program

The experimental program was conducted in the Structures Laboratory of the Department of Civil and Environmental Engineering at The University of Western Ontario. It involved six tests on full-scale rectangular RC beams that were designed so that their ultimate shear capacity was reached before their flexural failure.

3.2.1 Materials properties

A relatively low strength concrete (25 MPa) was selected for casting the beam specimens in order to emphasize the need for retrofit. The mix design of the concrete used was as follows: cement = 375 kg/m^3, coarse aggregate (well graded, 28-mm nominal maximum-size rounded gravel) = 1200 kg/m^3, fine aggregate (natural sand with an oven dry relative density of 2.64 and absorption of 0.7%) = 600 kg/m^3. The fineness modulus of the sand was 2.8 and the water to cement ratio (w/c) was 0.5. Cylindrical (150×300 mm) specimens were made to determine the compressive strength (ASTM C39) of concrete, f_c'. Splitting tests (ASTM C496) on cylindrical specimens were also used to measure the splitting tensile strength of the concrete, f_{ct}. The following average values were obtained at 28 days: cylindrical compressive strength of the concrete, f_c' = 25.1 MPa, splitting tensile strength, f_{ct} = 2.5 MPa. The Young's modulus (ASTM C469) was measured as E_c = 223 GPa and the Poisson's ratio (ASTM C469) under uniaxial compression loading was ν_c = 0.2.

The tensile strength of the reinforcing steel, f_y was 465 MPa. Its Young's modulus, E_s and passion ratio υ_s, were 200 GPa and 0.3, respectively. The properties of the FRP sheets used in this study are shown in Table 3.1. Mechanical properties of FRP laminates can be measured following the ASTM D-3039 standard guidelines.

The Tyfo epoxy, which is a two-component material product of Fyfe Company, was used for bonding the FRP sheets to concrete. Its viscosity at room temperature was between

600 cps to 700 cps. The Glass transition temperature, T_g of the epoxy was 82 °C measured following the ASTM D-4065 guidelines. The minimum tensile strength of the epoxy was 50.0 MPa (7.2 ksi), its ultimate elongation capacity was 5%, and it had a tensile modulus of elasticity of 3.18 GPa (461 ksi) measured according to the ASTM D-638 standard provisions.

3.2.2 Specimen preparation

Six identical size wooden frames were constructed and used to cast the concrete beams using the same ready mix concrete batch. Geometrical details of beams were selected by reviewing previous research and also considering the lab limitations. In Table 3.2, geometric details of the specimens are shown. Beams were overdesigned for flexural capacity and transverse steel was used at only one side of the beams to ensure that a shear failure will occur at the other side. In Fig. 3.1, the load scheme and configuration of the transverse and longitudinal steel are shown. The rectangular cross-section of beams has overall dimensions of 150 × 250 mm (5.9 × 9.8 in.).

The beams were smoothed at their edges to eliminate stress concentration effects and to improve the FRP/concrete bondline properties. Two control (not strengthened) RC beam specimens were labeled As-built-1 and As-built-2. All other beam specimens were retrofitted using parallel FRP schemes on two sides for each beam. Two beams were retrofitted using a hybrid composite scheme of Carbon-Glass and Carbon-Aramid (B-Π-CG, B-Π-CA). One beam was retrofitted using a unidirectional carbon fibre fabric (B-I-

C) with an inclination $\alpha = 90$ degrees to ensure interception of diagonal cracks. The last beam was retrofitted using $+45^{o}/-45^{o}$ glass fibres (B-III-GG). Dimensions and typical laminates details for the shear strengthening of all retrofitted RC beam specimens are shown in Fig. 3.2.

The concrete surface was prepared and made smooth and even before attaching the fibre-reinforced polymer sheets. Small voids on the surface of the RC beams were filled using ordinary cement grout. Using a two-component resin epoxy, the concrete/FRP bondline achieved adequate mechanical properties. Hence, in the numerical modeling, a perfect bond between the concrete and FRP sheets was assumed. Epoxy was combined with the FRP fabrics using the wet-layup method. Approximately 0.8 pounds of epoxy per 1.0 pound of fabric was used.

3.2.3 Loading apparatus and testing

The mechanical load was applied using a 250 kN capacity hydraulic jack. The various signals from the instruments were captured and monitored using an automated data acquisition system. Vertical displacements under the applied load were measured using linear variable differential transducers (LVDTs). Strains in the FRP sheets were also measured in three different directions to be able to calculate deformations in the crack zones and to compare the ultimate strain at failure and the effect of transverse fibres on the ultimate strain of the main vertical fibres. In Fig. 3.3, the instrumentation of the RC beam specimens is illustrated.

To apply quasi-static cyclic loading and to divide the load between two points, a rigid steel beam was utilized on top of the concrete beam. The steel beam was attached to the concrete beam using two steel plates with dimensions of 203×76×38 mm (8.0×3.0×0.5 in.) at the top and bottom of the beams. The steel plates were connected to each other using eight steel rods with a diameter of 12.7 mm (0.5 in.). In Fig. 3.4, the experimental set up and loading cross-section are shown. To prevent the vertical displacement of beams in two directions at the supports, two steel beams were attached vertically on top of the RC beam and connected to the strong floor. The loading was applied in a deflection control manner. The first cycle of loading had a deflection of ±3 mm in the actuator, so that the beam experiences both compression and tension. The actuator displacement frequency was set at 0.005 Hz throughout the test. For every other cycle, the amplitude of the actuator displacement had an increment of 3 mm both in the tension and compression zone. Each loading cycle was repeated three times to ensure a stable behaviour.

3.3 Numerical Analysis

The finite element program ABAQUS (version 6.6, 2006) was used to model the behaviour of the RC beams under monotonic loading up to failure and to predict their ultimate load capacity. Since the experimental loading was quasi-static, monotonic loading can reasonably simulate the overall behaviour of the beam. For instance, the force-displacement diagram of the beam in the monotonic state is the envelope of the quasi-static diagram in the compressive section. Five beams, one control RC beam and

four beams with different externally bonded FRP layers were considered in the numerical analysis.

3.3.1 Materials Properties and Constitutive Models

The materials used in the numerical analysis are concrete, steel and FRP. The constitutive models for the behaviour of these materials are presented below:

3.3.1.1 Steel

The steel rebar is assumed to have an elastic perfectly plastic behaviour as shown in Fig. 3.5. In ABAQUS, the steel reinforcement is treated as an equivalent uniaxial material smeared throughout the element section and can be defined alone or embedded in oriented surfaces. In order to properly model the constitutive behaviour of the steel reinforcement, the cross-sectional area, spacing, position and orientation of each layer of steel bar within each element needs to be specified. In the present model, two surface sections were defined for the top and bottom rebars with one layer of rebar in each surface. Steel ties were defined in surface sections using the same approach. These surfaces were embedded in the concrete section. Material parameters for steel rebars were obtained from experimental data as discussed earlier in section 3.2.1.

3.3.1.2 Concrete

Damage plasticity was used to model the concrete. It is a continuum, plasticity-based damage model for concrete, which uses concepts of isotropic damage elasticity in

combination with isotropic tensile and compressive plasticity to represent the inelastic behaviour of concrete. The model assumes that the main two failure mechanisms are tensile cracking and compressive crushing of the concrete material. Beyond the failure stress, the formation of micro-cracks is represented macroscopically with a softening stress-strain response, which induces strain localization in the concrete structure.

The inputs for the model are the compressive and tensile stresses of the concrete along with damage parameters in terms of plastic strains. The concrete strain, ε_o corresponding to the peak stress, f_c' is usually in the range of 0.002–0.003. A representative value suggested by the ACI Committee 318 and used in the analysis is ε_o = 0.003. For the compressive behaviour of concrete, the stress–strain relationship proposed by Saenz (1964) was used, and the softening branch was assumed to be linearly decreasing from 23 MPa to 2 MPa (from ε_c = 0.003 to ε_c = 0.01) (Fig. 3.6).

$$\sigma_c = \frac{E_c \varepsilon_c}{1+(R+R_E-2)\left(\frac{\varepsilon_c}{\varepsilon_o}\right)+(2R-1)\left(\frac{\varepsilon_c}{\varepsilon_o}\right)^2+R\left(\frac{\varepsilon_c}{\varepsilon_o}\right)^3} \tag{3.1}$$

Where

$$R = \frac{R_E(R_\sigma - 1)}{(R_\varepsilon - 1)^2} - \frac{1}{R_\varepsilon}, R_E = \frac{E_c}{E_o}, E_o = \frac{f_c'}{\varepsilon_o} \tag{3.2}$$

and $R_\sigma = 4$, $R_\varepsilon = 4$.

The tensile strength of concrete is typically 8-15% of its compressive strength. A value of 2.5 MPa measured from the splitting tensile test was used. The softening part of the tensile stress-strain curve is modeled by two lines as shown in Fig. 3.6.

Plasticity parameters were defined in ABAQUS. The damage plasticity model in ABAQUS requires the following parameters to be defined: yield and failure surfaces (Table 3.3.). In Table 3.3, f_{bo} is the biaxial compressive strength, and f_{co} is the uniaxial compressive strength used to define the yield and failure surfaces. K is the ratio of the second stress invariant on the tensile meridian, to that on the compressive meridian. The model also needs damage evolution in terms of plastic strain; this data was obtained from report by Jankowiak et al. (2005). Moreover, it was assumed that concrete recovers 95% of its strength in compression after initial damage.

3.3.1.3 FRP

FRP layers were modeled using membrane elements. FRP was considered to be orthotropic and elastic. Since FRP layers generally behave differently in three orthogonal directions, an orthotropic elastic constitutive model was used. It was also assumed that non-linear behaviour of FRP is negligible. Since no bending was assumed for FRP layers, simple planar membrane elements were used. Bonding between FRP and concrete was simply modeled by constraining membrane elements to brick elements. The material parameters for FRP sheets were obtained from experimental data.

3.3.2 FEM model

Since the RC beams were not symmetric, they had to be modeled over their entire length. Concrete was modeled using ordinary 8-noded solid brick elements with 3×4×50 mesh ties. Steel rebars were modeled using surface elements, while FRPs were modeled by membrane elements. Explicit dynamic approach was selected and the problem was solved in a displacement control manner. In order to simulate quasi-static loading, a one-*cm* displacement was applied in 10 seconds. Since modeling was based on monotonic loading, two beams were modeled for each experimental beam, one for compressive loading and the other for tensile loading (Fig .3.7).

3.4 Results and Discussion

3.4.1 Experimental

In all tests, no major cracks were observed until near the ultimate load. However, as illustrated in Fig. 3.8 the effect of stress concentration at the steel plates contact surface with concrete led to separation of some concrete due to the bearing stress before failure occurred. As expected, failure occurred at the side of the beam with no transverse steel. Beams had lower deflection and higher force for the same amount of actuator displacement in the compression zone with respect to the tension zone. This shows the importance of the shear span ratio and longitudinal rebar effect on the structural behaviour of concrete beams, because except for the longitudinal steel rebar sizes, the beams were symmetric at the top and bottom. Concrete crashed at the compression zone where no steel ties were used, and longitudinal steel rebars did not yield throughout the

experiment. Loading was done using incremental amplitudes of the actuator displacement (±3mm; ±6mm; etc.). Each cycle, except the last one, was repeated thrice to model the effect of repetitive loading. Figure 3.9 shows the cyclic loading pattern versus loading time, while, Fig. 3.10 shows the displacement versus time at the center of all beams during the testing. Figure 3.11 shows the load-deflection (P/δ) hysteretic curves at mid span of the beam specimens. The ductility of all specimens was improved slightly after being retrofitted. The maximum compressive and tensile values of strains at different locations, and load versus deflection values were summarized in Table 3.4.

The control beams without FRP sheets had an average ultimate failure load of 91.6 kN (20.6 kips) in tension, and 145.7 kN (32.1 kips) in compression, respectively (values of the ultimate load capacity of these two beam specimens were comparable with only 5% difference). Shear cracks developed suddenly at the maximum shear span at about 45° inclination, followed by a sudden shear failure in the weak side of the beam specimen as illustrated in Fig. 3.12. Failure occurred at the second cycle of the last amplitude of actuator movement (±12mm). Some small cracks became visible at the first cycle of the last amplitude, but no major cracks were observed.

Various retrofit protocols consisting of four strips of i) carbon/epoxy, ii) carbon-glass/epoxy, and iii) carbon-aramid/epoxy hand layup systems, were applied to the treated shear span concrete surfaces of beams designated as B-I-C, B-II-CG and B-II-CA, respectively. Although the main strengthening material, CFRP, is brittle in nature, previous work has shown that increasing the ductility of RC beams in which CFRP has

been used for strengthening can be achieved [12]. Beam B-I-C failed at the first cycle of the ±15mm actuator load, while beams B-II-CG and B-II-CA failed at the actuator load of ±18mm. Beam B-II-CA achieved the best performance. Its ultimate compression capacity increased by 35% compared to the measured value for the control RC beam specimens. The ultimate failure mode of the retrofitted specimens was a typical concrete crushing. Shear cracks initiated at the un-strengthened areas of the shear span. The failure angle changed from 45 degrees for the control beam to 55 degrees, and the third FRP sheet got separated from the RC beam along with a relatively thick concrete layer. Failure was brittle and accompanied by a loud sound. By comparison of the maximum compression and tension values of strains of beams retrofitted by hybrid FRP sheets (B-II-CG, B-II-CA) with the observed values for beam B-I-C which had only unidirectional carbon fibres, it can be concluded that the hybrid application of FRP sheets increased the chance of rupture at the main fibres and allowed them to contribute more shear capacity. Figure 3.13(a, b) illustrates the failure of beam specimens B-I-C and B-II-CG.

A repair technique consisting of four strips of glass-glass/epoxy hand layup system was applied to the treated shear span concrete surfaces of the beam designated as B-III–GG. Bidirectional glass fibres in the -45° and +45° directions were applied for retrofitting this beam. The ultimate capacity of the repaired beam was 163.8 kN (36.1 kips) in compression and 94.3 kN (20.8 kips) in tension, which indicates that the glass-glass/epoxy hand layup system effectively improved the shear strength of the original beam by up to 12% in compression. The failure angle was approximately 45 degrees and the third FRP sheet ruptured. The lower thickness and strength of glass FRP sheets

compared to that of the carbon FRP sheets used for the other beams allowed fibres to reach their maximum strain capacity and experience rupture instead of de-bonding. Figure 3.13c illustrates the shear failure of the B-III-GG beam specimen.

3.4.2 Numerical model

3.4.2.1 As-built shear beam specimens

The first model predicted cracking load in compression for the original beam was 43.4 kN, which is 1% lower than the corresponding experimental value (44.0 kN). Figure 3.11a shows that in compression the post cracking behaviour, i.e. when cracks propagate in the beam and the beam's response becomes non-linear, is well described by the numerical model, since the numerical values form the envelope for the experimental values and the overall error is negligible. The ultimate load in compression was estimated to be 173 kN, which is 20% larger than the observed value. This appears to be due to fatigue loading and the existence of micro-cracks in the original specimen. These aspects were not considered in the FEM model. The maximum displacement in the tension side was 8.3 mm, which is 11% higher than the experimental value of 7.4 mm. The predicted tensile cracking load was 27.5 kN, which is 10% less than the corresponding experimental value. The predicted ultimate load in tension was 82.3 kN, which is 10% less than the experimental value of 91.6 kN. The cracking pattern in compression is illustrated in Fig. 3.14a which shows that the main cracks are due to shear and appear at 45 degrees in the beam side where there were no ties. Moreover, some flexural cracks appeared, which were small and not visible in Fig. 3.14a.

3.4.2.2 Specimens with CFRP at main direction

Carbon/epoxy repair evaluation Specimen (B-I-C)

In compression, the model prediction is in reasonable agreement with experimental data in the elastic range. The cracking load was 36 kN, which is 15% lower than the observed value. The ultimate load was 173 kN and the maximum displacement was 9.5 mm, which are 4% and 29% larger than the corresponding experimental values (Fig. 3.11b). In tension, the model prediction was in general agreement with the experimental data. The cracking load was 36 kN which is 10% above the measured value. The ultimate load was 86 kN, and sudden collapse was observed when the steel rebars started to yield. Figure 3.14b shows that the cracking pattern was changed compared to that of the As-built beam due to the existence of external FRP sheets and a wider area of concrete has cracked compared to that of the control RC beam, which shows that the external FRP increased the ductility. It can also be observed that the area between the second and third FRP sheets was critical since more cracks were observed in this region.

Carbon/Glass/Epoxy and Carbon-Aramid/Epoxy retrofit scheme (Specimens B-II-CG, B-II-CA)

Model predictions for these beams were in a very good agreement with experimental data in the elastic range. The post cracking trend agrees well with experimental observation in the compression and tension zones (Fig 3.12. (c, d)). It can be observed in Fig 3.14. (c, d)

that, FRP has changed the cracking pattern in the beams compared to that of control beam. FRP increased the cracking area, and the zone between the second and third FRP sheets was critical area and failure happened there. This observation is compatible with experimental observations where the third FRP sheet was debonded from the beam. Moreover, these beams experienced higher maximum strain compared with that of B-I-C. The maximum strain experienced by FRP sheets to retrofit beams B-II-CG and B-II-CA were 28% and 37% higher compared to that of B-I-C at failure. This experimental and numerical observation proves that hybrid application of FRP sheets and application of glass and aramid fibres at transverse direction has significant effect on shear capacity contributed by FRP sheets. Beside shear cracks, some flexural cracks were also observed at the bottom of the beams.

3.4.2.3 Glass-Glass/epoxy repair evaluation (Specimen B-III-GG)

In compression, the model predictions were in a good agreement with the corresponding experimental data in elastic range. The cracking load was 36 kN, which is 16% below the measured value. The post-cracking trend was also compatible with experimental data (Fig. 3.11e). Figure 3.14e shows the strain distribution and crack pattern for beam specimen B-III-GG. The numerical analysis continued beyond experimental observation, considering the stresses induced in the FRP in Fig. 3.15, the beam would have failed at an ultimate load of 198 kN, which is 20% above the corresponding experimental value. The model predicts the rupture of the third FRP sheet at the weak side of the beam, which is compatible with experimental observation. In tension, the model predicted the elastic

behaviour very well; the cracking load was 35 kN, which was the same as the measured experimental value, the post cracking trend was also in excellent agreement with experimental observations. The ultimate load was 86.4 kN, which is 8% below the corresponding experimental value.

3.4.3 Hybrid FRP effect

Debonding of FRP sheets does not allow such sheets to contribute their maximum capacity to the ultimate shear load of RC beams. Generally, the application of most mechanical anchors or bolts to prevent this debonding has not been successful, mainly because of stress concentration effects (Barnes *et al.* 2006). The present study shows that the hybrid application of FRP sheets increases the confinement of fibres in the main direction, and consequently the entire FRP laminate shows better stress-strain behaviour and debonding of the FRP sheets can be postponed.

Research was done by Sakar *et al.* (2009) on the effect of bidirectional CFRP sheets for retrofitting reinforced concrete (RC) beams under cyclic loading. They concluded that adding a horizontal ply in the 0^{o} direction helped to increase the shear friction strength and hindered the crack development at the tension face. Moreover, hybrid application of FRP sheets helped to increase the contribution of the concrete to shear resistance by postponing the crack propagation at the concrete surface.

The ultimate shear resistance of beams with carbon fibres at main direction was compared to the nominal shear resistance predicted by the Colotti model (2004) to clarify the effect of hybrid application of FRP sheets. As expressed before current codes and models ignore effect of fibres at transverse direction. The ultimate shear capacity in compression of all of tested beams at this research with carbon fibres at main direction (B-I-C, B-II-C, B-II-CA) was calculated as 159.8 kN using Colotti model (eq. 2.17 to eq. 2.23). As observed also by Mosallam et al. (2007), the Colotti model gave relatively accurate prediction for the beam retrofitted by unidirectional FRP sheets as external reinforcement (B-I-C) with an error of 4% compared to 166.2 kN experimental observation. While, errors for the beams with hybrid FRP sheets (B-II-CG, B-II-CA) are 12% and 27%, respectively, compared with 178.4 kN and 196.8 kN experimental results.

In addition to ignoring the effect of the transverse fibres, it is not guaranteed that carbon fibres, concrete and/or steel stirrups will make use of their maximum strength at the failure of the beam. Common design codes, however, still use the relative contribution of these materials to calculate the total shear strength. It should be also pointed out that the mechanisms by which concrete, steel and FRP contribute to the overall shear capacity interact with each other.

More recently, Galal *et al.* (2009) proposed a new mechanical anchoring method which is claimed to eliminate the debonding of epoxy-bonded carbon fibre-reinforced polymer (CFRP) sheets, thus utilizing the full capacity of dry carbon fibre sheets. In this method, dry carbon fibre sheets are wrapped around and bonded to two steel rods. Then the rods

are anchored to the corners of the web-flange intersection of a T-beam with mechanical bolts. This makes a U-shaped dry carbon fber jacket around the web, which increases the shear strength of the T-beam using the the higher tensile strength and modulus of elasticity of the dry CF compared to that of the composite CFRP. This method is more labor intensive compared to the application of epoxy for bonding FRP to concrete. Moreover, it is generally applicable for beams with T-sections.

3.5 Concluding Remarks

The objective of the experimental program and numerical analysis in the present study was to evaluate the ultimate shear strengths and to identify the modes of failure of a control RC beam, along with that of unidirectional and hybrid FRP retrofitted beam specimens under quasi-static cyclic loading. The following conclusions can be drawn based on the experimental and numerical work discussed in this chapter:

(i) Hybrid FRP sheets showed a better performance in increasing the ultimate shear capacity of RC beams compared with that of unidirectional carbon fibre-retrofitted beam specimens. The co-existence of other fibres like glass or aramid in the transverse direction allowed carbon fibres in the main direction to get closer to its ultimate strain capacity.

(ii) As shown in previous work (Colotti *et al.* 2005), RC beams with thicker two sides laminated FRP sheet are less likely to undergo failure by rupture of the FRP sheet. Beam B-III-GG, which had glass with lowest thickness as

external FRP, was the only specimen which had FRP rupture at failure. The numerical analysis confirmed this behaviour.

(iii) Design codes and current models need to incorporate provisions that consider the effect of hybrid FRP sheet applications and the interaction between the shear capacity contributed by the FRP sheets and that by concrete.

(iv) The Colotti model provides accurate estimation of the shear capacity of RC beam specimens retrofitted using unidirectional fibres. However, it had a considerable error in calculating the shear capacity of beams retrofitted with hybrid FRP sheets.

(v) Different structural behaviour of RC beams in tension and compression loading confirmed the importance of *a/d* and the longitudinal rebar effect on the shear behaviour of RC beams. This aspect has been generally ignored by several design codes and needs further research.

(vi) Fatigue and repetitive loading affect the ultimate capacity of RC beams through the formation of micro-cracks in concrete and weakening of the bonding layer between concrete and the external FRP sheets. This effect needs to be quantified and accounted for in cyclic loading.

Table 3.1: Details of FRP strengthened RC beam specimens

Specimen	FRP	t_f, mm	E_{f1}, GPa	f_{fu1}, MPa	E_{f2}, GPa	f_{fu2}, MPa	α , degree
B-I-C	Carbon	1.00	87.3	925	3.2	72.4	90°
B-П-CG	Carbon-Glass	1.00	95.8	986	49.3	270.2	0° /90°
B-П-CA	Carbon-Aramid	1.00	72.4	876	61.5	290.3	0° /90°
B-Ш-GG	Glass-Glass	0.25	19.3	309	19.3	309.0	-45° /+45°

Table 3.2: Details of RC beam specimens

Specimen*	b, mm	d, mm	Tension Steel, mm	ρ	Compression Steel, mm	ρ'	Stirrup, mm	Stirrup, Spacing, mm	ρ_w	a/d	FRP
As-Built-1	150	220	2φ11	0.003	3φ16	0.009	6	150	0.003	2.5	-
As-Built-2	150	220	2φ11	0.003	3φ16	0.009	6	150	0.003	2.5	-
B-I-C	150	220	2φ11	0.003	3φ16	0.009	6	150	0.003	2.5	90° C
B-П-CG	150	220	2φ11	0.003	3φ16	0.009	6	150	0.003	2.5	90° /0° C-G
B-П-CA	150	220	2φ11	0.003	3φ16	0.009	6	150	0.003	2.5	90° /0° C-A
B-Ш-GG	150	220	2φ11	0.003	3φ16	0.009	6	150	0.003	2.5	-45° /+45° G-G

* C = carbon, G = glass, A= aramid

Table 3.3: Damage parameters in plasticity model used for concrete

Dilation angle	Eccentricity	f_{bo}/f_{co}	K	Viscosity parameter
40	10	1.16	0.667	0

Table 3.4: Experimental results of shear capacity of FRP retrofitted RC beam specimens

Specimen	Compression					Tension				
	Force, (kN)	Displacement ' (mm)	Strain			Force (kN)	Displacement (mm)	Strain		
			0	45	90			0	45	90
As-Built	145.7	7.3	-	-	-	91.6	8.2	-	-	-
B - I- C	166.2	6.9	0.003	0.010	0.009	88.8	9.82	0.002	0.006	0.005
B-П-CG	178.4	9.6	0.005	0.012	0.011	92.8	13.2	0.003	0.005	0.005
B-П–CA	196.8	11.9	0.007	0.014	0.012	94.8	16.5	0.003	0.005	0.005
B-П–GG	163.8	6.2	0.010	0.017	0.013	94.3	13.4	0.002	0.007	0.006

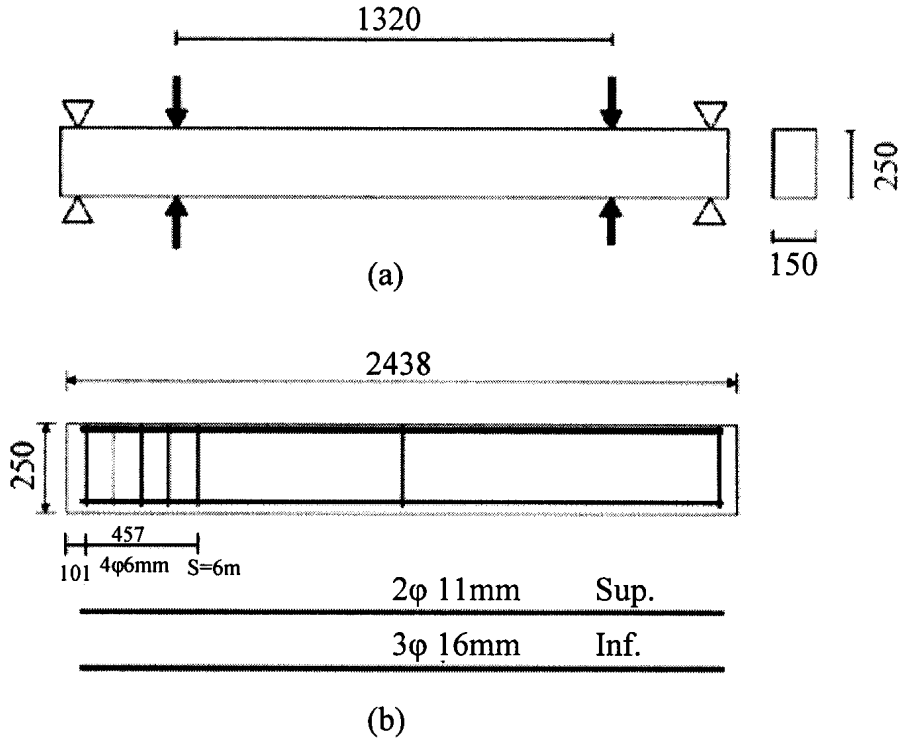

Fig. 3.1: Load scheme and configuration of transverse and longitudinal steel.

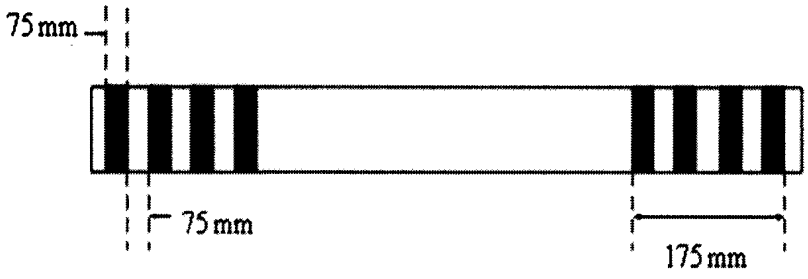

Fig. 3.2: Typical shear strengthening details.

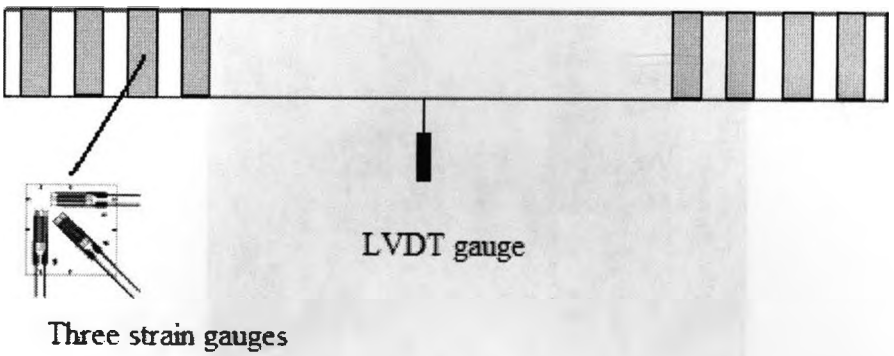

Fig. 3.3: Instrumentation of strain gauges at 0/45/90 degree on the third FRP sheet and location of LVDT gauge.

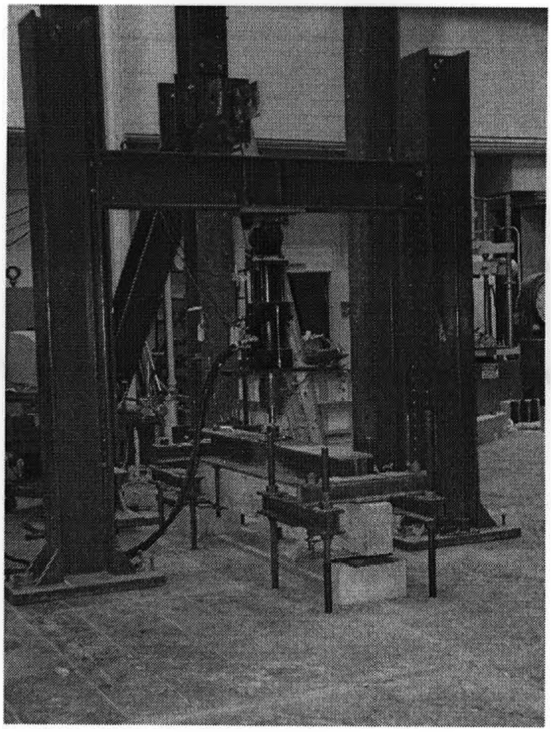

(a)

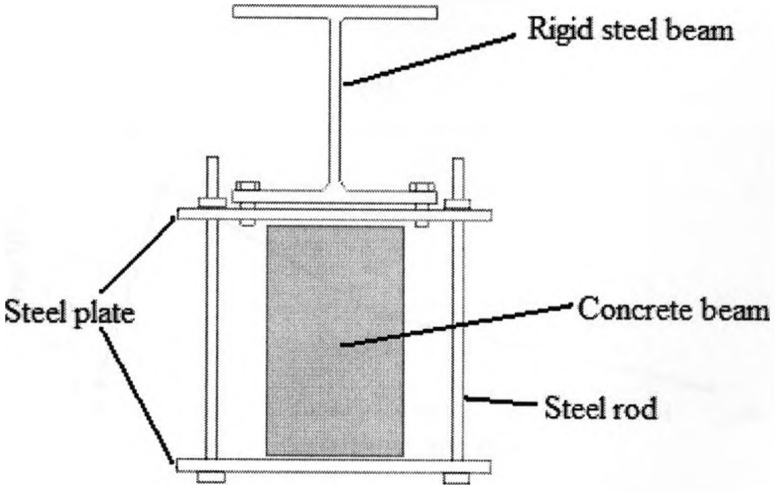

(b)

Fig. 3.4: (a) Experimental set up, and (b) loading cross-section.

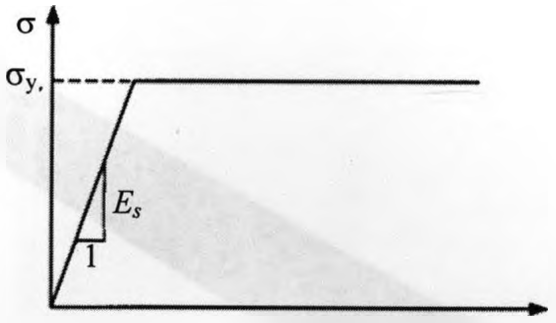

Fig. 3.5: Stress-strain relationship for steel.

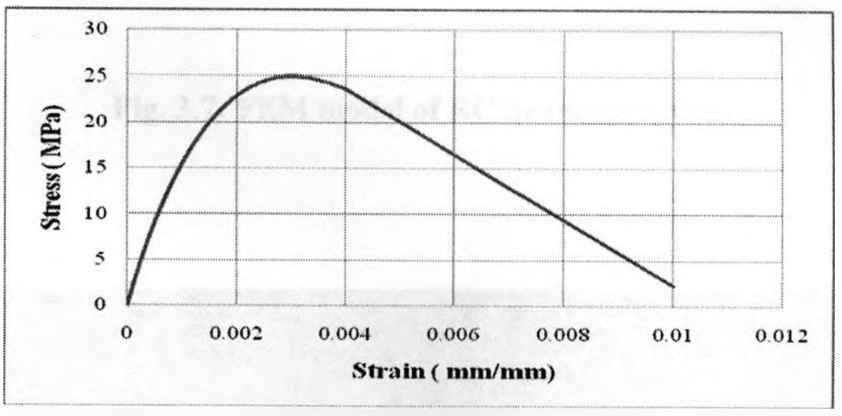

(a)

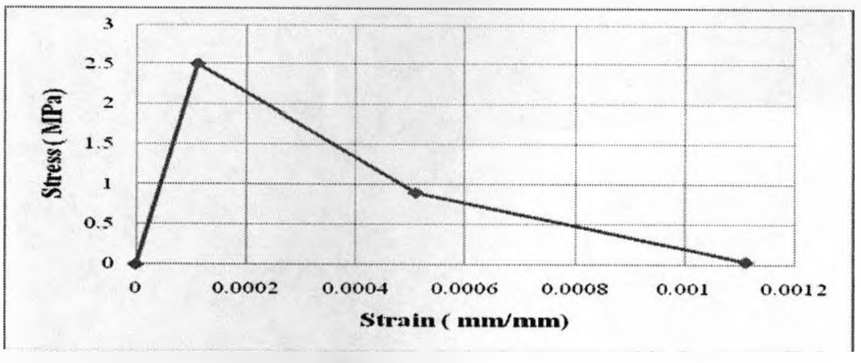

(b)

Fig. 3.6: (a) Compressive behaviour of concrete used in FEM model, and (b) Tensile behaviour of concrete used in FEM model.

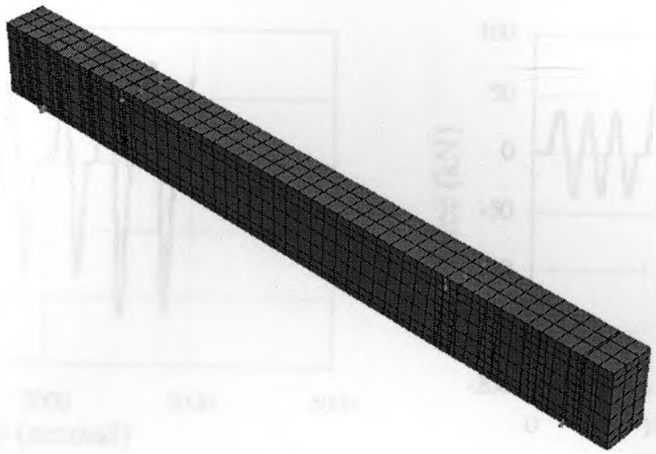

Fig. 3.7: FEM model of RC beam specimens.

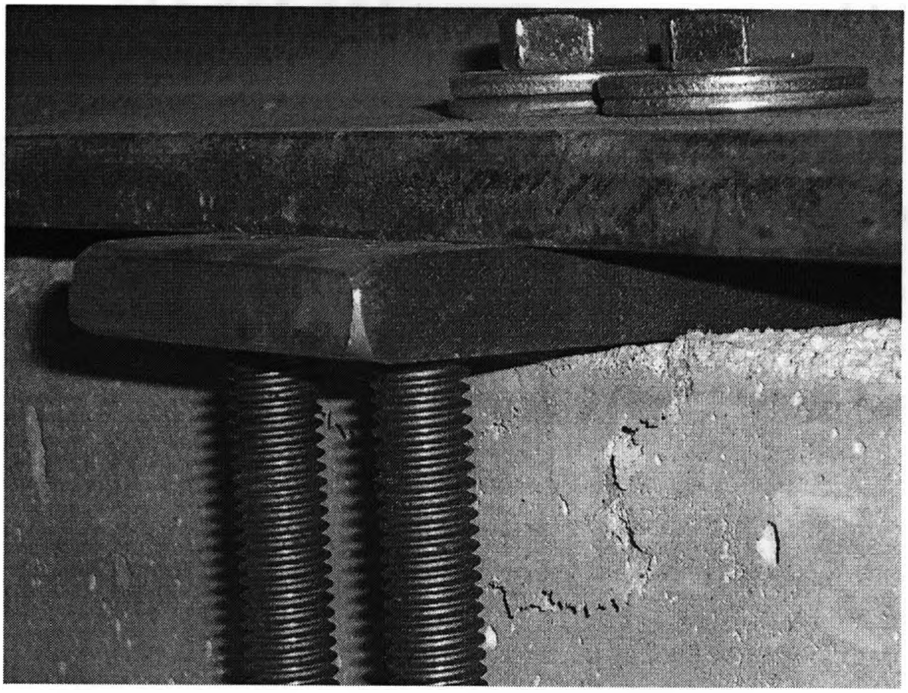

Fig. 3.8: Bearing stress effect on contact surface of steel and concrete.

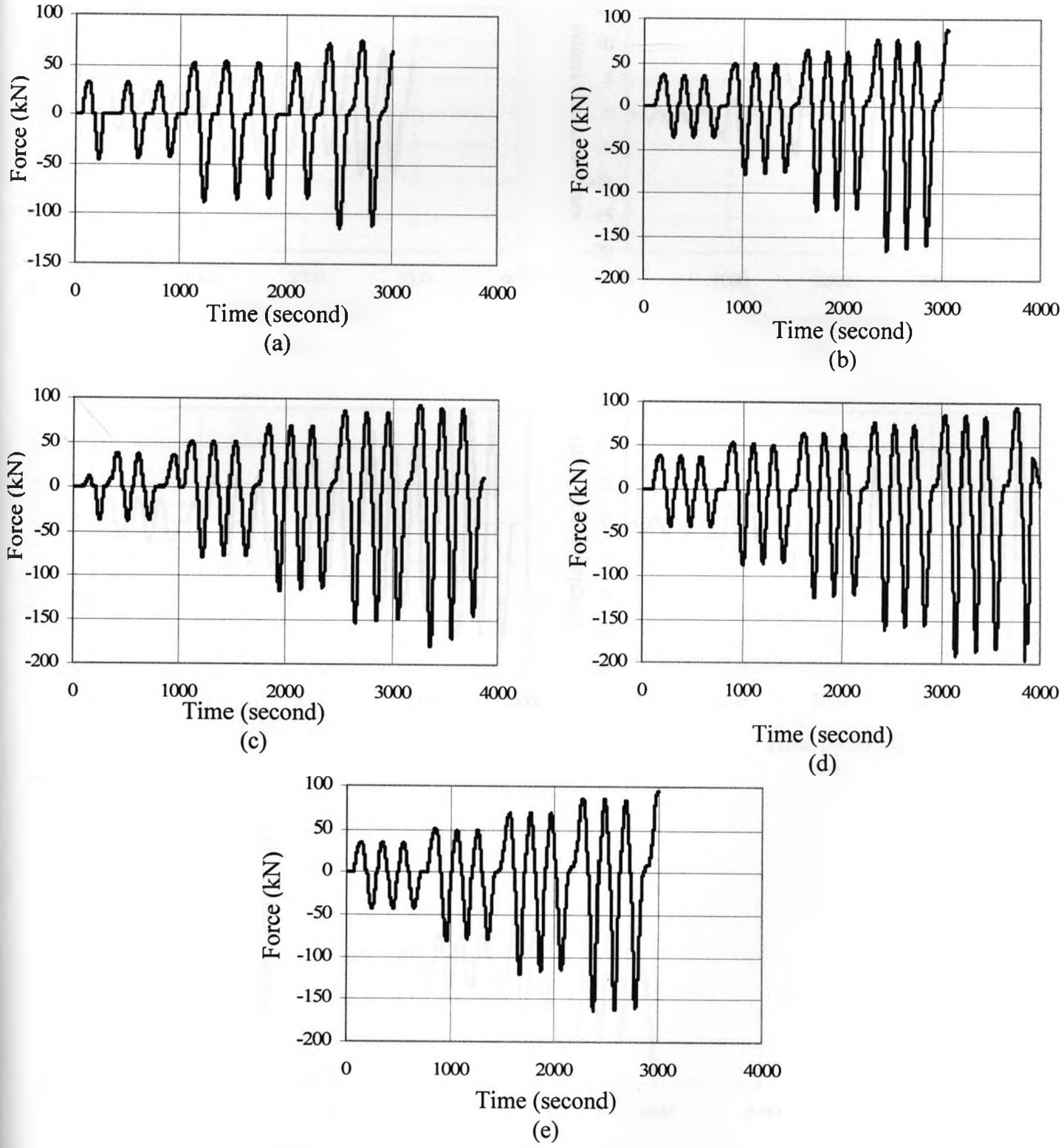

Fig. 3.9: Force – time diagram for (a) control RC beam specimen, (b) B-I-C specimen, (c) B-II-CG specimen, (d) B-II-CA specimen, and (e) B-III-GG specimen, respectively.

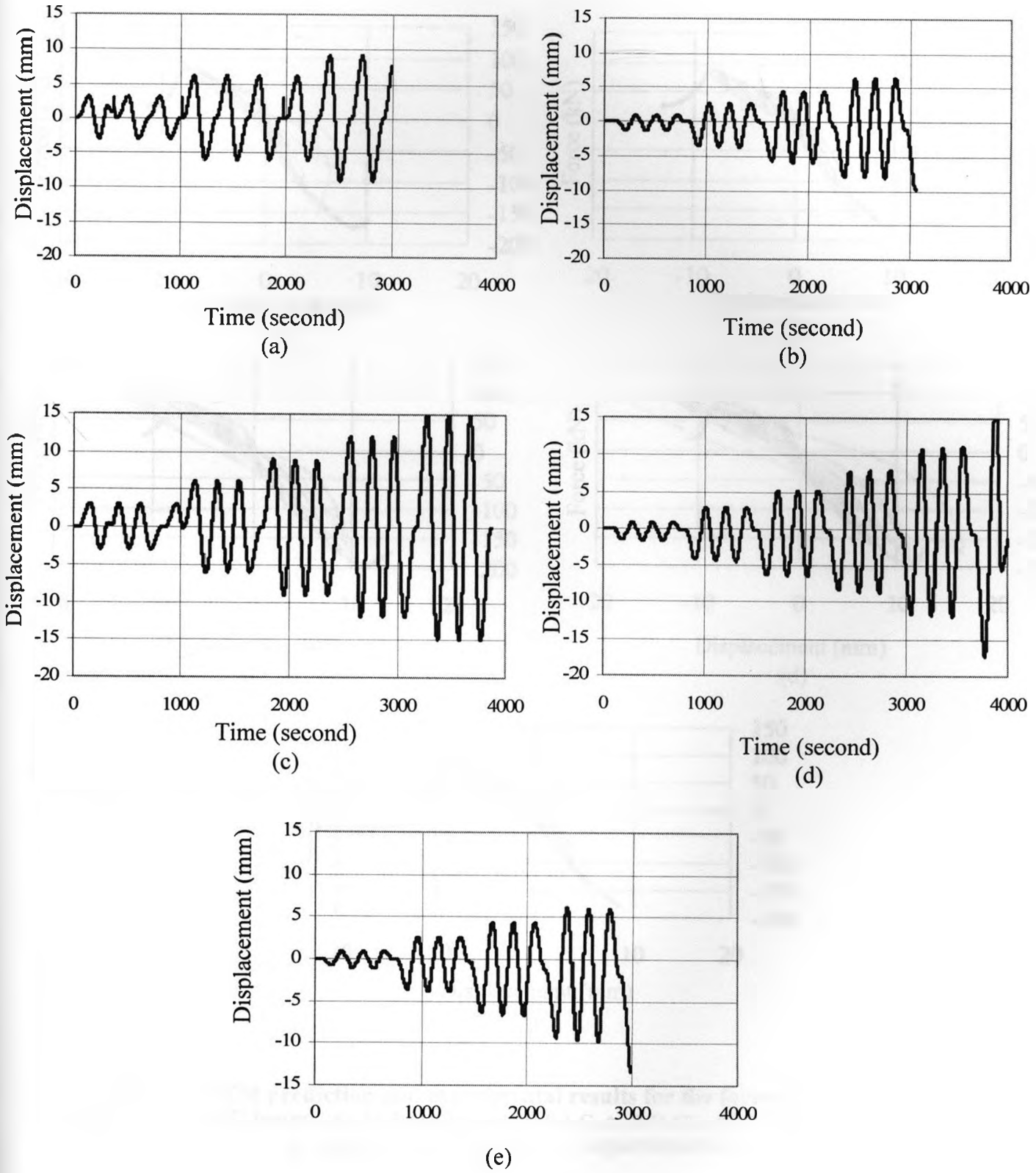

Fig. 3.10: Displacement at the center of the beam versus time diagram for (a) control RC beam specimen, (b) B-I-C specimen, (c) B-II-CG specimen, (d) B-II-CA specimen, and (e) B-III-GG specimen, respectively.

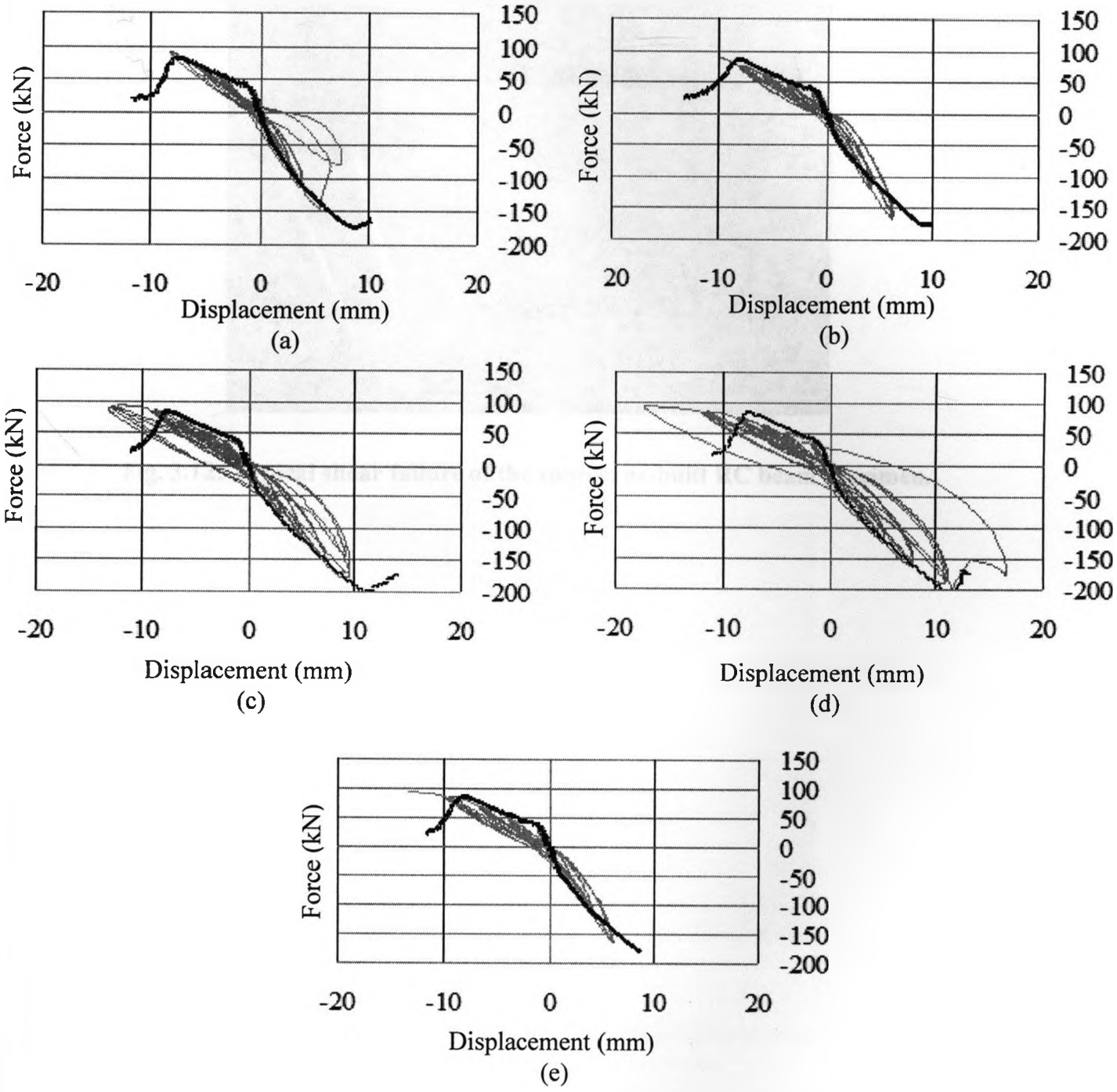

Fig. 3.11: FEM prediction and experimental results for the force-displacement behaviour of RC beams, a) As-built beam, b) B-I-C, c) B-II-CG, d) B-П-CA, and e) B-Ш-G. (▬▬ Numerical, ____ Experimental).

Fig. 3.12: Typical shear failure of the control as-built RC beam specimen.

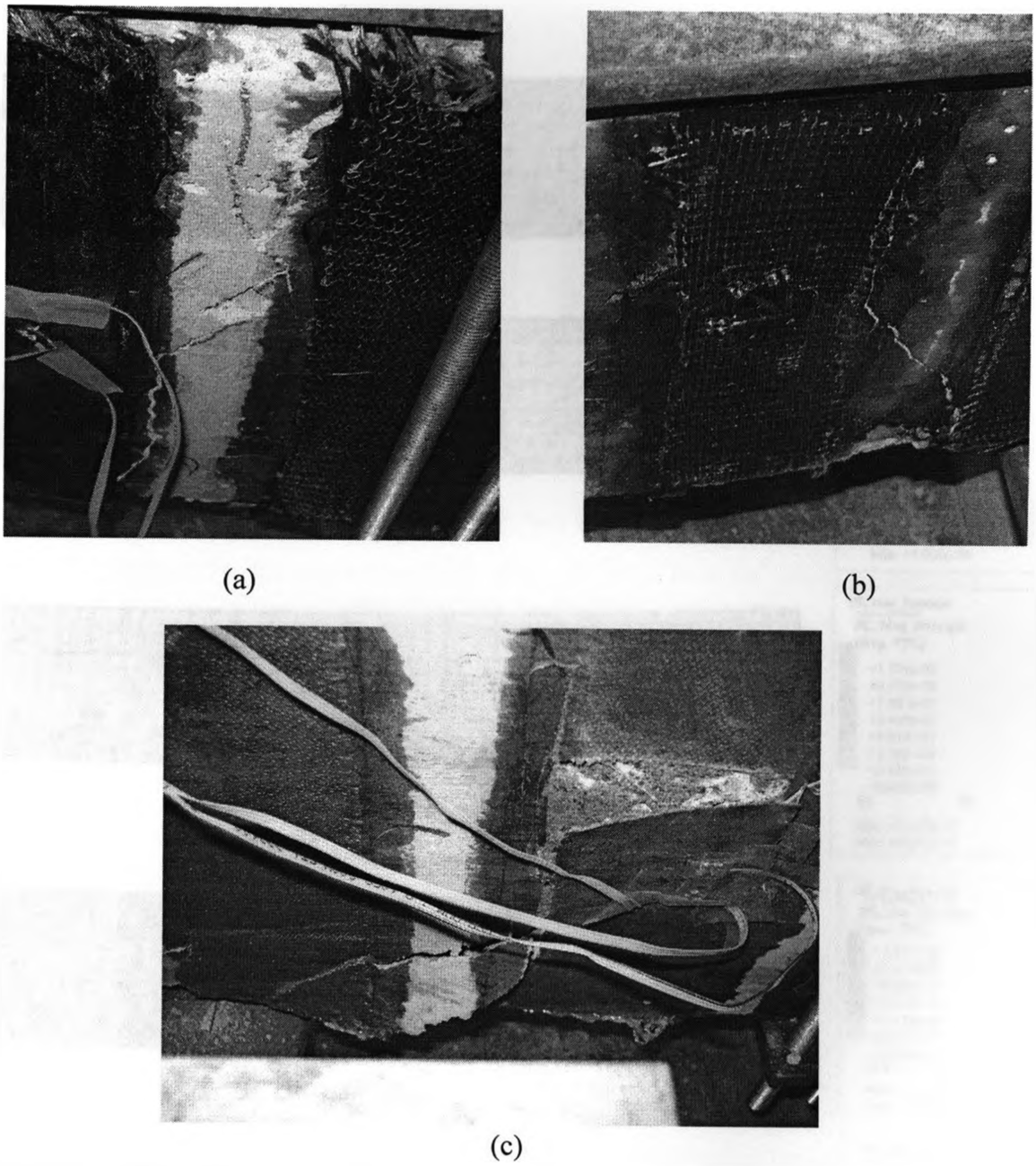

Fig. 3.13: Shear failure and crack pattern for (a) B-I-C specimen, (b) B-П-CG specimen, and (c) B-Ш-GG specimen.

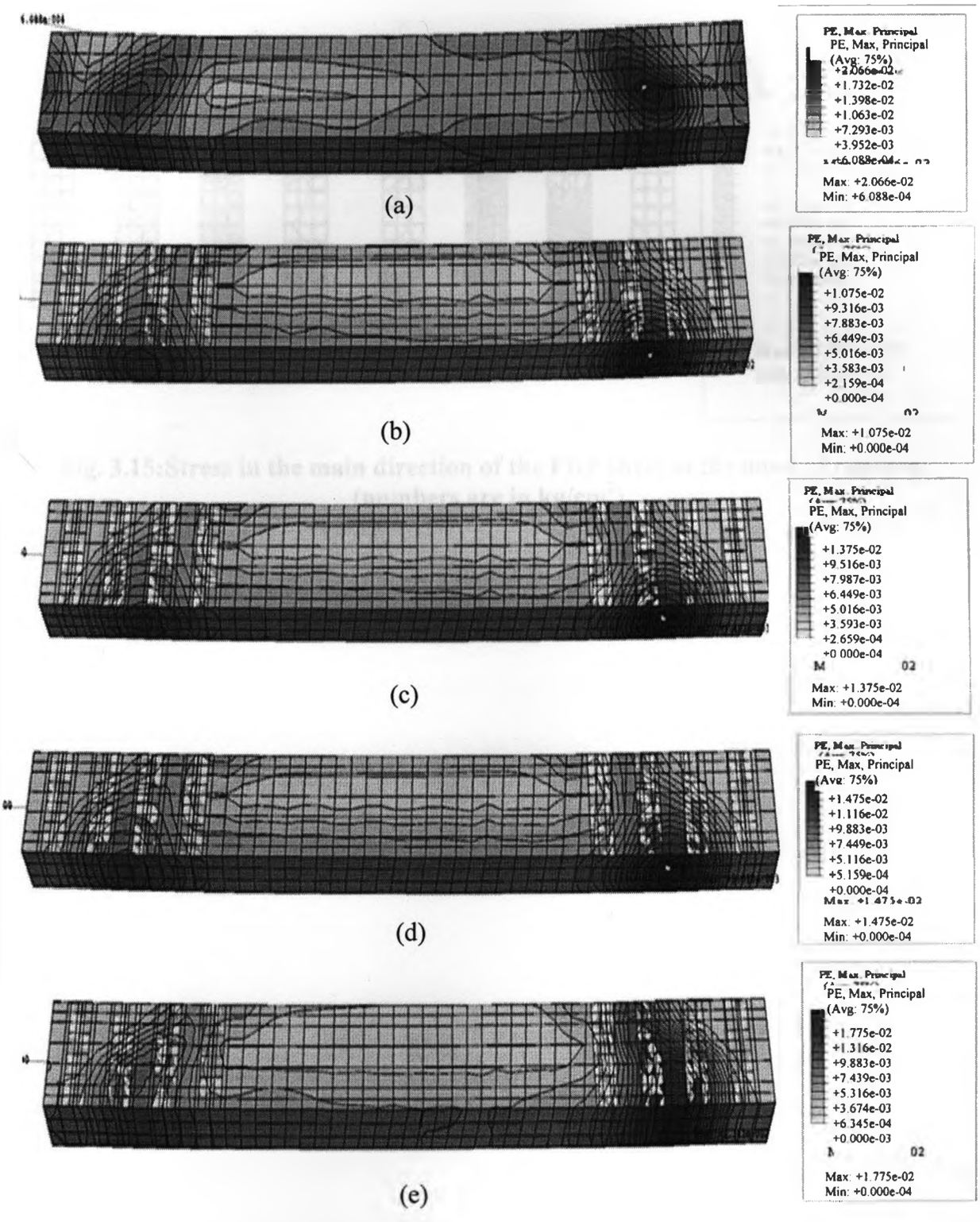

Fig. 3.14: FEM results for the maximum principal plastic strain contour for RC beam specimens, a) as-built beam, b) B-I-C, c) B-П-CG, d) B-П-CA, and e) B-Ш-G.

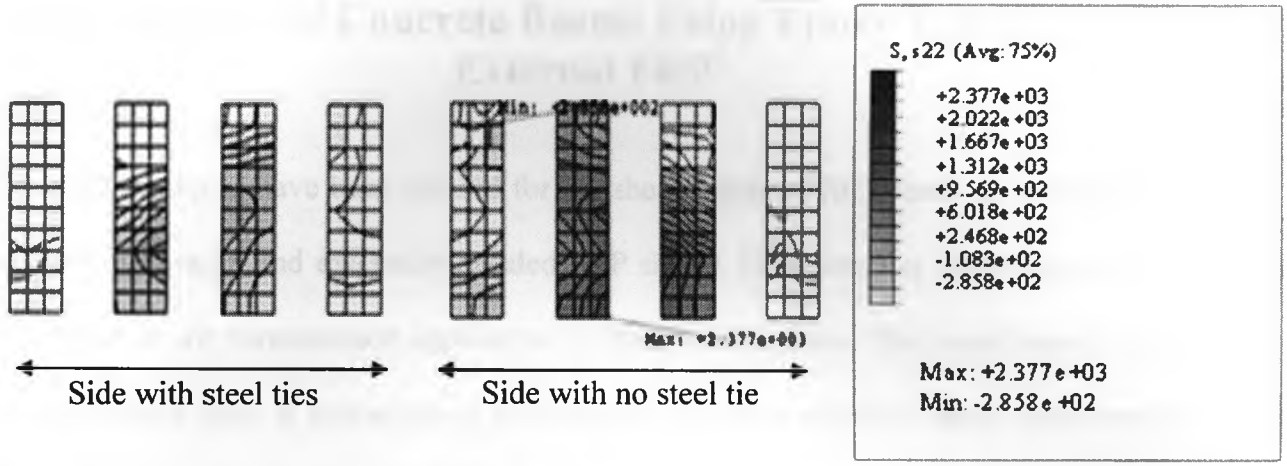

Fig. 3.15:Stress in the main direction of the FRP sheet at the onset of rupture (numbers are in kg/cm^2).

CHAPTER 4

Shear Repair of Concrete Beams Using Epoxy Injection and External FRP[2]

Several techniques have been utilized for the shear repair of RC beams including epoxy injection of cracks and externally bonded FRP sheets. However, not much research has been done on the simultaneous application of these two methods. This experimental study at this chapter aims at investigating performance of beams repaired using simultaneous epoxy injection and external FRP sheets under monotonic loading. Three severely damaged beams were repaired using epoxy injection and unidirectional carbon fibre polymer (CFRP) sheets. The repairing method, FRP type, and wrapping scheme were test variables investigated in this experimental program. Test results show that the repair schemes imparted significant mechanical improvements in terms of ultimate shear capacity and ductility. The simultaneous application of epoxy injection and externally bonded FRP sheets was found to be highly effective repair technique. Failure type of beam is also highly dependent on application scheme of external FRP sheets.

4.1 Introduction

Repair and rehabilitation work for concrete structures can broadly be classified into two main categories: (i) repair in which the damage due to deterioration and cracking is corrected to restore the original structural capacity, and (ii) repair that is necessary to

[2] A version of this chapter has been submitted for review to ACI Materials Journal

strengthen the structural capacity of a member whose load carrying capacity has either been inadequate or whose strength has been severely impaired (Al-Gadhib et al., 2003).

Epoxy resins are commonly used repair materials that generally have very good bonding and durability characteristics (ACI Committee 546R-96, 1996). Calder and Thompson (1998) reported that the overall structural performance of RC slabs repaired using epoxy resin injection performed best compared to other repair materials such as polyester and methyl methacrylate resins. The stiffness of the cracked slabs in this study was about one quarter of that of the un-cracked slabs and the repairs reinstated only about half of the stiffness loss. According to Minoru et al. (2001), the bond between concrete and the injection material is very critical; a good bond may restore the original stiffness of the repaired material and prevent further penetration of chloride ions and water. The crack should also be clean and dry prior to injection. Epoxy injection is not applicable if the cracks are actively leaking or cannot be dried out, unless moisture tolerant epoxies that can flush the moisture from the inner crack surfaces are used.

The American Concrete Institute (ACI) Guide 440.2R-02 (2002), shows that cracks wider than 0.25 mm can move and may affect the performance of externally bonded FRP systems through delamination or fibre crushing. Small cracks exposed to aggressive environments may require resin injection to improve durability performance and delay corrosion of existing steel reinforcement before FRP strengthening.

The present study is undertaken to enhance the understanding of how epoxy injection affects the shear behaviour of reinforced concrete beams with and without CFRP fabrics subjected to four-point static loading. Three of the damaged which were tested on the previous study in chapter three were repaired using epoxy injection into the cracks, two of the beams also had additional new external FRP sheets on its damaged shear span. All three beams were subjected to normal monotonic loading up to failure.

4.2 Experimental Program

In this experimental work, three damaged beams which were tested at previous phase (presented at the chapter three) were repaired using epoxy injection and retested.

4.2.1 Materials properties

Characteristic of concrete, steel, FRP sheets and epoxy used to bind the concrete and external FRP sheets was the same a previous chapter (section 3.2.1).

A two-component epoxy was used to seal crack surfaces in damaged beam specimens and to attach injection ports to the concrete beams. It had a tensile strength of 31.0 MPa, an elongation at break of 0.5%, compressive yield strength of 96.5 MPa determined as the ASTM D-638 "Standard Test Method for Tensile Properties of Plastics" standard provisions. The bond strength between the concrete and this epoxy was 15.9 MPa as

determined following the ASTM C882 "Standard Test Method for Bond Strength of Epoxy-Resin Systems Used with Concrete by Slant Shear" testing procedure.

Another two-component low-viscosity epoxy adhesive (product of BASF chemical company) was used to inject cracks in the damaged concrete beams. It had a tensile strength of 52.0 MPa, an elongation at break of 1.0%, and a compressive yield strength of 76.0 MPa determined following the ASTM D-638, "Standard Test Method for Tensile Properties of Plastics" standard testing guidelines. The bond strength between concrete and this epoxy was 14.0 MPa as per the ASTM C882, "Standard Test Method for Bond Strength of Epoxy-Resin Systems Used with Concrete by Slant Shear" testing recommendations.

4.2.2 Specimens preparation

Three of the damaged beams (presented at chapter three) after quasi-static loading were subsequently repaired using epoxy injection. The As-built-1 control RC beam specimen was repaired using epoxy injection only and labeled "As-built-R". Beam B-I-C, which had unidirectional carbon fibre fabric, was first prepared by removing damaged FRP sheets, repaired using epoxy injection, and then the same scheme of unidirectional carbon fibres was applied. The repaired beam was labeled "B-I-CR1". The As-built-2 control RC beam specimen was also repaired using epoxy injection, and then all shear span surfaces were covered using external unidirectional carbon fibres. The repaired beam was labeled "B-I-CR2". The epoxy injection repair was carried out as follows: first, cracks were

cleaned thoroughly with compressed air. Injection ports were then installed using surface sealing epoxy. The ports were spaced 15 cm apart and were applied on both sides of the beam. Cracks were sealed with epoxy in order to retain the injected epoxy (Fig. 4.1a.). The injection process was started after the sealing epoxy cured. The epoxy injection was initiated at the lowest port until it reached the port above. The lowest port was then capped. The process was repeated until the epoxy completely filled all cracks and all ports were capped. Epoxy injection was done using injection guns (Fig. 4.1b.). After curing of the epoxy, the ports were removed, and the seals were grinded off. After surface preparation, CFRP sheets were applied to the surfaces of beam specimens B-I-CR1 and B-I-CR2 as discussed above. Figure 4.2 shows typical shear strengthening details used in used for B-I-CR1 and B-I-CR2 shear specimens. Table 4.1 shows details of strengthened specimens and FRP sheets used.

4.2.3 Loading apparatus and testing procedure

The same testing set up as presented in previous chapter was used except with difference that bottom plates and connection rods were removed and monotonic loading was applied to the beam specimens. Figure 4.3 shows the loading set up for B-I-CR2. The load was applied using a relatively low displacement rate of 0.5 mm per minute.

4.3 Results and Discussion

4.3.1 Results for repaired beam specimens

Experimental results of ultimate load capacity and displacement obtained on testing repaired beams have been summarized in Table 4.2. The load versus mid-span displacement for repaired beams is presented in Fig. 4.4.

4.3.1.1 "As-built-R" shear beam specimen

This beam specimen was only repaired using epoxy injection into cracks. It exhibited an ultimate load capacity of 176.4 kN, which was 21% higher than the ultimate capacity of the "As-built" control beams. The final displacement of the specimen was 13 mm, which was 78% greater than that of the "As-built" control beam. This indicates that the epoxy injection repair protocol was very effective both in terms of load capacity and ductility improvements. Also, in the linear part of the deflection-force graph, higher stiffness was observed compared to that of the control beam. This could be explained by the bond-strength to concrete of the low viscosity injection material which was higher than the tensile strength of the concrete itself. Hence, new cracks formed next to the injected ones at the weakened locations. The beam failed by concrete crushing at the side of the beam which had no stirrups. However, major cracks were also observed at the side with transverse steel rebars. Figure 4.5a shows the "As-built-R" repaired specimen crack pattern at failure.

4.3.1.2 B-I-CR1 beam specimen

In addition to repairing cracks with epoxy injection, this beam specimen had four unidirectional CFRP laminates on each of its shear spans. There was a free space between subsequent laminates equal to the width of each laminate (75 mm) (Fig. 4.2a.). The beam had an ultimate load capacity of 233.0 kN, which is 33% higher than that of the repaired specimen "As-built-R" and 40% higher than that of the retrofitted specimen B-I-C presented earlier. Again, this can be due to the higher bond strength between the concrete and the injected epoxy compared to the tensile strength of the concrete. The final midspan displacement of the beam was 7.7 mm, which is 41% lower than that of the repaired "As-built-R" beam, but 19% higher than that of the retrofitted specimen B-I-C tested in the previous phase. Comparing the ultimate deflection of the this beam with that of the repaired specimen "As-built-R" indicates that some FRP repair schemes can increase the ultimate shear capacity but reduce ductility. Higher ductility of this specimen compared to that of the retrofitted specimen B-I-C can be justified by the formation of a plastic hinge at the injected epoxy location.

This beam behaved almost linearly up to its brittle failure. The beam specimen with epoxy crack injection had a higher initial stiffness than that of the counterpart specimen without epoxy injection. Major cracks were also observed at the side of the beam having transverse steel ties. However, the beam failed at the side with no transverse steel as expected. Contrary to the behaviour observed in the previous phase, FRP sheets ruptured

in the repaired beam specimen and the crack angle was almost 45°. The crack pattern at failure for beam B-I-CR1 is illustrated in Fig. 4.5b.

4.3.1.3 B-I-CR2 beam specimen

In this beam, all shear spans were completely covered using unidirectional CFRP sheets (Fig. 4.2b.) subsequent to low epoxy injection of cracks. There was a significant improvement in the mechanical behaviour of this specimen, particularly in its ultimate midspan displacement capacity and much enhanced ductile behaviour. The ultimate capacity of the B-I-CR2 beam specimen was 192.5 kN, which is 9% higher than that of the "As-Built-R" specimen. The ultimate midspan deflection of the beam at failure was 29.3 mm, which is 125% higher than that of the "As-Built-R" specimen. Comparing the ultimate deflections of beams B-I-CR1 and B-I-CR2 shows that a ductile or brittle behaviour of the repaired beams is highly dependent on the scheme used for external FRP rehabilitation, which can shift a very brittle failure to a ductile one.

First major cracks during the loading of this specimen occurred at the end of the FRP sheets on the concrete surface where both shear and moment loads are considerably high while no retrofit or repair protocol was applied at that location. As observed in Fig. 4.4, at the initial elastic zone, the beam showed similar behaviour to that of the "As-Built-R" beam specimen with approximately the same stiffness. However, it could undergo much higher deflection at the plastic zone with an almost constant load of 190 kN. A crash of concrete occurred in the shear span of the beam at the beam side having no transverse

steel reinforcement, which led to debonding of the attached FRP laminate. The crack pattern and failure of beam B-I-CR2 is illustrated in Fig. 4.5c. It can be argued that epoxy injection of cracks aided in limiting crack opening. Moreover, epoxy injection combined with externally bonded FRP sheets was very effective for the structural repair of shear deficient RC beams.

4.3.2 Comparison with conventional repair methods

Historically, intact concrete members have been retrofitted by post-tension or jacketing with new concrete in conjunction with a surface adhesive (Klaiber, 1987). Since the mid 1960's, epoxy bonded the steel plates have been used in Europe and South Africa to retrofit concrete members (Dussek, 1987). Steel plates have a durability problem unique to this application, because corrosion may occur along the adhesive interface. This type of corrosion adversely affects the bond at steel plate-concrete interface and is difficult to monitor during routine inspections. Additionally, special equipment is necessary to install the heavy plates. As a result of these problems new materials have been sought by engineers. Unidirectional or woven FRP laminates have proven to be a promising alternative for retrofitting exiting RC structures. However, results of the first phase of the presented experimental study showed that the application of hybrid FRP sheets has a considerable effect on improving the mechanical behaviour of the retrofitted beams in terms of ultimate shear capacity and ductility improvements compared to that of unidirectional FRP.

Several methods have also been used for repairing cracks in damaged RC beams, including, (i) routing and sealing, (ii) drilling and plugging, and (iii) stitching which can be performed by drilling holes on both sides of the cracks and grouting a U-shaped steel stitch with epoxy. The main disadvantage of the routing and sealing method is that not much load capacity can be reinstated in the structural member, while the main difficulty in using the drilling and plugging or stitching technique is that they are more labor intensive. Moreover, a high amount of stress concentration usually occurs at the concrete surface using these methods (Hamoush, 1997). The application of epoxy injection generally eliminates such problems.

The simultaneous application of epoxy injection and externally bonded FRP sheets for repairing damaged RC beams was observed to be highly effective. Repairing cracks using epoxy injection improve not only the short term, but also the long term behaviour of damaged beams by reducing chloride ion and moisture migration to longitudinal rebars. Moreover, the injected epoxy can have better mechanical characteristics than concrete, such as higher tensile and better elongation strength than original concrete. Simultaneous application of FRP sheets with epoxy injection increases the confinement of the concrete section, and has demonstrated effectiveness in the shear repair of RC beams in the present study.

4.4 Concluding Remarks

The objective of this experimental study was to evaluate the ultimate shear strength and to identify the modes of failure of re-retrofitted beams using epoxy injection or epoxy injection combined with externally bonded CFRP laminates. The following conclusions can be drawn based on the experimental results discussed in this chapter:

(vii) Crack injection using low viscosity epoxy provided an increase of stiffness in the linear region of the load-displacement curves of all repaired RC beams tested in the second phase of the testing program.

(viii) An increase in the ultimate strength of all beams was observed in the second phase of testing compared to their counterparts in the first phase. This is likely due to the stronger epoxy to concrete bond-line strength compared to the tensile strength of concrete.

(ix) Whether to observe ductile or brittle behaviour of RC beams repaired with epoxy injection and external FRP sheets is highly dependent of the scheme and type of the attached FRP laminates.

Table 4.1: Details of strengthened specimens and FRP sheets used

Specimen	FRP	t_f, mm	E_{f1}, GPa	f_{fu1}, MPa	E_{f2}, GPa	f_{fu2}, MPa	α , degree
B-I-CR1*	Carbon	1.00	87.3	925	3.2	72.4	90°
B-I-CR2	Carbon	1.00	87.3	925	3.2	72.4	90°

*Shear span surfaces were totally covered by CFRP in B-I-CR2 while half of the surface area was covered in B-I-CR1

Table 4.2: Experimental results of shear capacity of retrofitted beam specimens

Specimen	Loading	Results	
		Force, (kN)	Displacement, (mm)
As-Built-R	Monotonic	176.4	13.0
B - I- CR1	Monotonic	233.0	7.7
B - I- CR2	Monotonic	192.5	29.3
As-Built	Cyclic	145.7	7.3
B - I- C	Cyclic	166.2	6.9

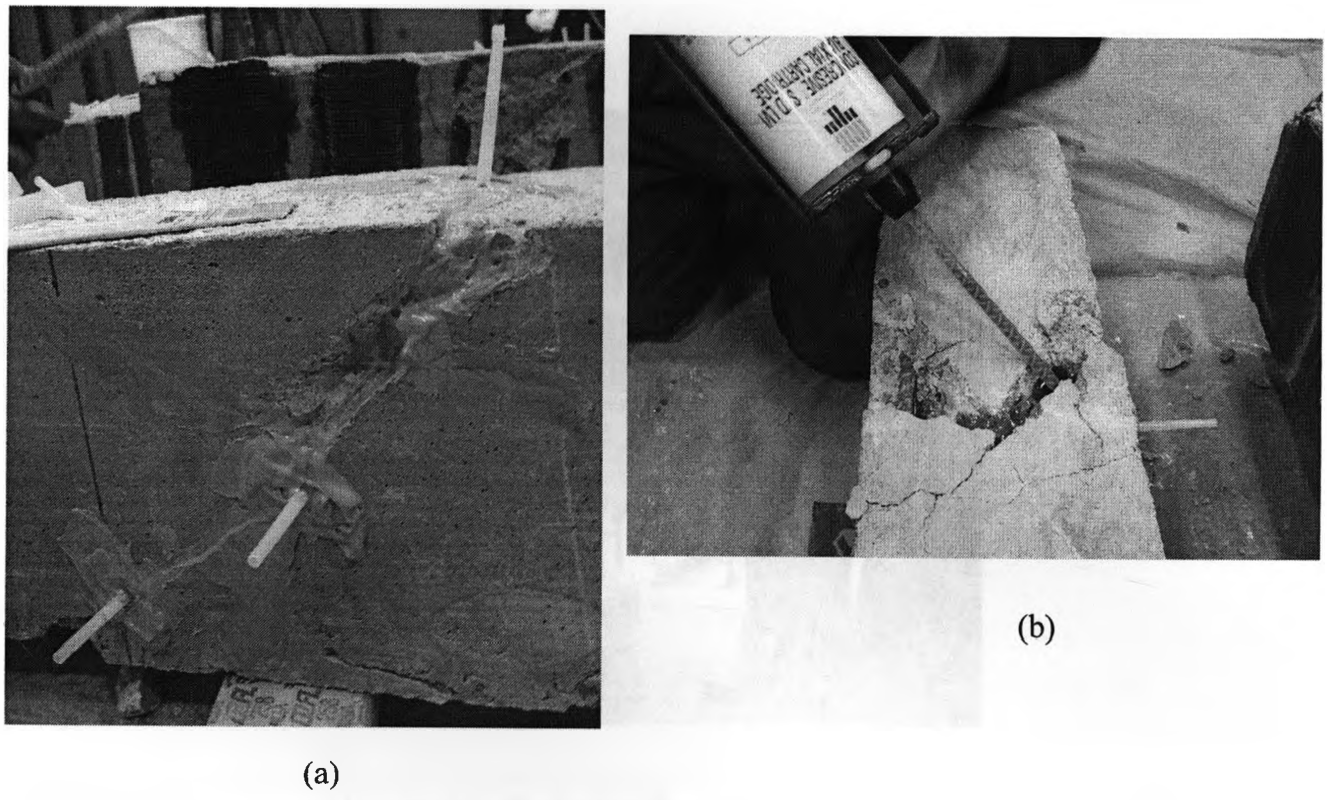

(a) (b)

Fig. 4.1: (a) Sealed surface and installed injection ports for the second phase of testing repaired beams, and (b) injection of epoxy into the cracks using an injection gun.

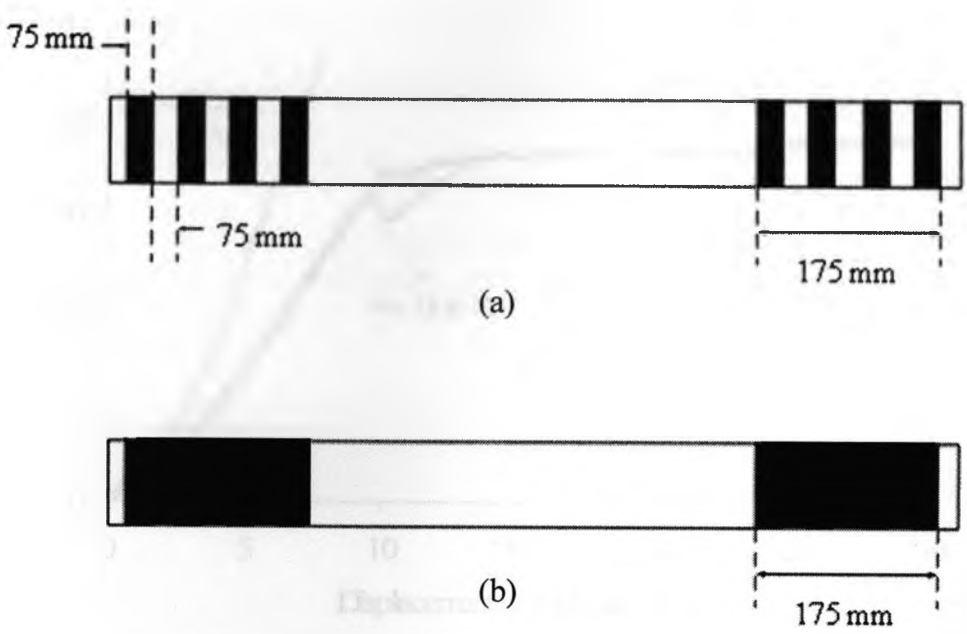

Fig. 4.2: Typical shear strengthening details used in, (a) B-I-CR1, and (b) B-I-CR1 shear specimen.

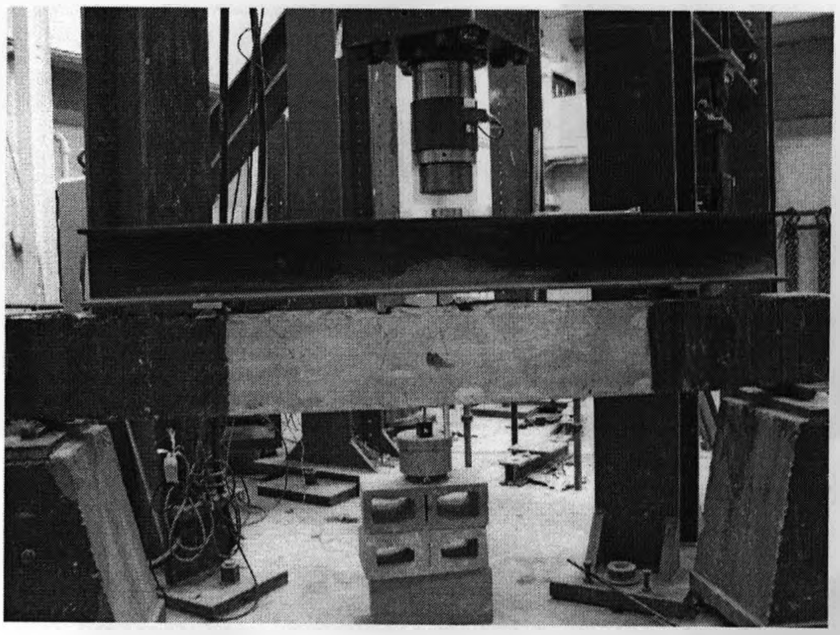

Fig. 4.3: Experimental set-up used in second experimental phase on repaired RC beams.

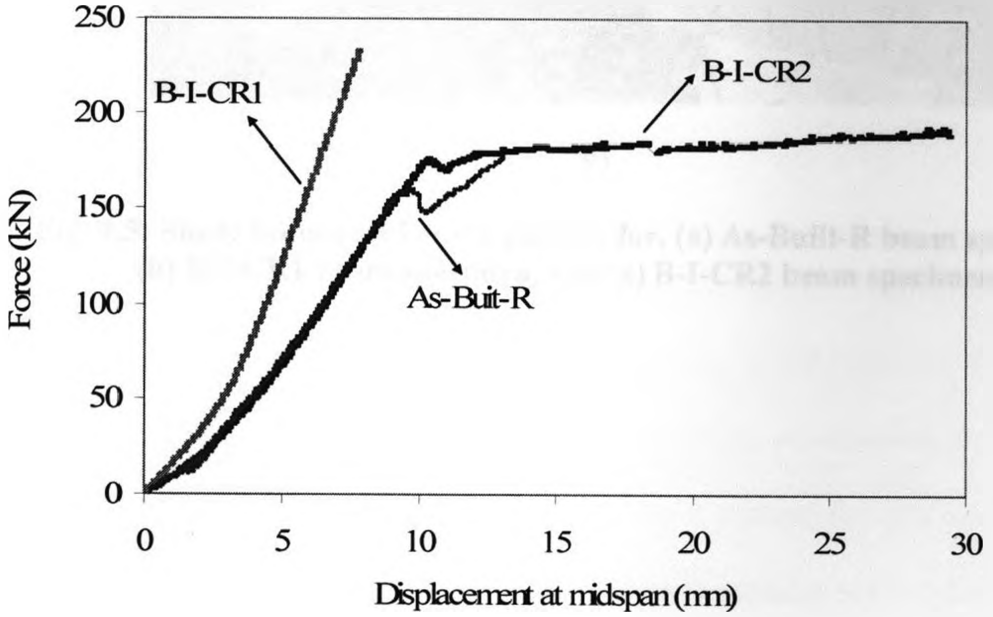

Fig. 4.4: Experimental results for force versus displacement at the midspan of the beams at the second phase of testing.

(a)

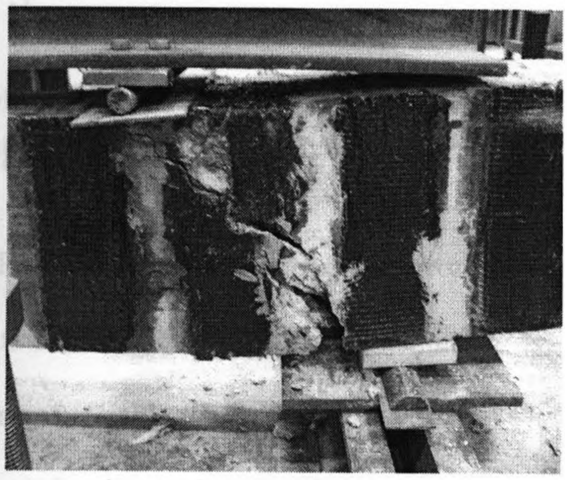

(b)

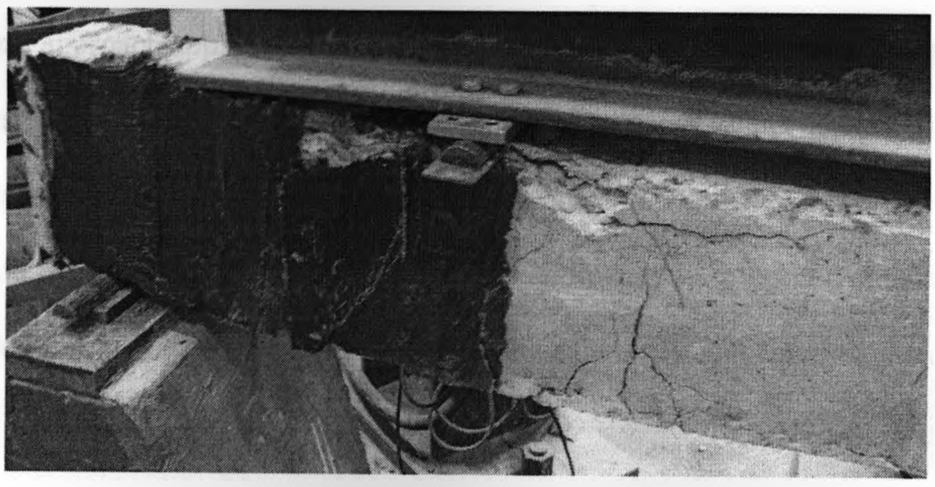

(c)

Fig. 4.5: Shear failure and crack pattern for, (a) As-Built-R beam specimen, (b) B-I-CR1 beam specimen, and (c) B-I-CR2 beam specimen.

CHAPTER 5

Modeling Shear Capacity of FRP Bonded-Reinforced Concrete Beams Using Genetic Algorithms Approach[3]

Although a variety of on-site applications using FRP materials have been realized world-wide, this technology is currently at a stage where its future wide-spread implementation and competitiveness will depend on the development of reliable design guidelines based on sound engineering principles. This chapter presents simple, yet improved, equations to calculate the shear capacity of FRP bonded-reinforced concrete beams based on the genetic algorithms approach applied to 212 experimental data points available in the open literature. The performance of the proposed equations was compared to that of commonly used shear design methods, namely the ACI 440, Eurocode (EC2), the Matthys Model, Colotti model and the ISIS Canada guidelines. Results show that the proposed equations better agree with the available experimental data than the existing models investigated.

5.1 Introduction

Previous studies (e.g. Mosallam *et al.* 2007) concluded that current design guidelines are highly conservative and underestimate the shear capacity of FRP-bonded RC beams. Accordingly, the objective of this study is to develop simple, yet accurate, shear design equations for FRP- bonded RC beams with and without stirrups for different kinds of FRP laminates and variable configurations. The proposed equations account for the effect of common shear design parameters and have been developed based on the genetic

[3] A version of this chapter has been submitted for review to Journal of Materials and Structures.

algorithms approach using the ultimate shear capacity results of 212 FRP- strengthened RC beams available in the open literature.

This work aims at improving the understanding of the complex mechanisms that characterize the ultimate shear capacity of continuous and simply supported RC members with transverse steel reinforcement and externally bonded FRP sheets. In particular, the mechanisms of interaction between the external FRP strengthening and the internal steel shear reinforcement and concrete strength are investigated. This interaction is generally not considered in design code provisions and in most existing shear design models, which generally assume that FRP strengthening does not change the shear resistance contributed by concrete and/or steel.

5.2 Genetic Algorithms Methodology

Genetic algorithms (GAs) are used in computing both exact and approximate solutions to optimization and search problems. Categorized as a global search experience-based technique, GAs are a particular class of evolutionary algorithms that use techniques inspired by evolutionary biology, including inheritance, mutation, selection, and crossover to solve problems. GAs have become increasingly useful in the nonlinear programming field as a result of their strong search capabilities.

GA is case dependent and the appropriate selection of its key parameters is essential for its successful development and acceptable performance. These key parameters include

the selection method and pressure, recombination type and rate, mutation rate and number of individuals. The selection method and pressure are critical in directing the search and arriving at an appropriate solution. Their operation depends on the nature and difficulty of the problem to be solved. The value of the recombination and mutation rates is essential to the convergence and stability of the solution. A high value of the crossover rate gives larger space for exploring possible solutions, allowing for the optimum solution to be found and reducing the possibility of the solution converging to a local optimum. One negative aspect is that a recombination rate that is too high may lead to a search of less-promising regions, delaying the convergence of a solution. A high mutation rate leads to more random alterations in which offspring start losing their resemblance to their parents. In contrast, a low mutation rate may cause the solution to try fewer individuals who would otherwise have been useful to the solution. More information about this issue is discussed by Goldberg (1989).

The genetic algorithms approach has several applications in engineering practice; however, the GA has not been used in concrete materials and structural research until recently. Ramasamy and Rajasekaran (1996) investigated the potential for using expert systems, artificial neural networks, and genetic algorithms, in order to construct an empirical model for the shear strength of reinforced concrete deep beams. Nehdi (2007) used the GA method to calculate the shear capacity of RC beams that are internally reinforced with FRP rebars. Genetic algorithms were also used in modeling the compressive strength of cement mortar (Akkurt *et al.* 2003) and in the design of the mixture proportions of high-strength concrete (Lim and Yoon 2004).

5.3 Experimental Database

In this study, the ultimate shear capacity for 212 RC beams were collected from published literature (Mosallam *et al.* 2007, Khalifa *et al.* 1999, Cao *et al.* 2005, Abdel-Jaber *et al.* 2003, Kachlakev *et al.* 1999, Kage *et al.* 1997, Mitsui *et al.* 1998, Sato *et al.* 1996, Triantafillou 1998, Uji 1992, Huthchinson *et al.* 1999, Taerwe *et al.* 1997, Taljsten *et al.* 1999, Michael *et al.* 1995, Carolin *et al.* 2005, Pellegrino *et al.* 2006, Hadi 2003, Monti *et al.* 2006, Matthys 2000, Spadea *et al.* 1998, Swamy *et al.* 1996, Norris *et al.* 1997, Umezu *et al.* 1997, Araki *et al.* 1997, Swamy *et al.* 1999, Chajes *et al.* 1995, Al-Sulaimani *et al.* 1994). A total of 132 data points had CFRP, 58 had GFRP and 22 had AFRP as externally bonded reinforcement. The database was complied in a patterned format. Each pattern consists of an input vector containing the geometrical and mechanical properties of the retrofitted RC beam, and an output vector containing the corresponding shear capacity. Table 5.1 shows the range of shear design parameters and ultimate shear capacity of beams used in the database.

5.4 Proposed Design Equation Based on Genetic Algorithms Model

In most of the previous empirical models, the following equation was adopted

$$V_{f,exp} = V_{u,exp} - V_{u,base} \tag{5.1}$$

Where, $V_{u,base}$ is the ultimate shear capacity of a similar beam but without any external FRP laminates. It has been shown by Pellegrino (2006) that there is considerable interaction between steel stirrups and external FRP laminates and that it is possible at

failure, whether in de-bonding or rupture, stresses in the steel stirrups be much lower than the yield stress.

The genetic algorithms approach has been used herein as an optimization technique to develop equations for the shear design of externally bonded FRP reinforced concrete beams with or without shear reinforcement. Thus, an original form of the equation defining the overall shear bahaviour and including the main shear design parameters that influence the shear capacity of concrete beams is required. The original form of the shear equations considered in the GA optimization are as follows:

$$V_n = (C_1\sqrt{f_c'} + C_2\frac{\rho_l}{\frac{a}{d}})b_w d + \frac{A_v f_{steel} d}{s} + \frac{A_f E_f \varepsilon_{fe} d_f}{s_f}(\sin\alpha + \cos\alpha) \quad (5.2)$$

$$\varepsilon_{fe} = C_3 \Gamma_f^{C_4} \varepsilon_u \quad (5.3)$$

$$\Gamma_f = \frac{E_f \rho_f}{f_c^{\frac{2}{3}}\left(a/d\right)} \quad (5.4)$$

$$\rho_f = \frac{A_f}{b s_f} \quad (5.5)$$

$$f_{steel} = \min(\varepsilon_{fe} E_s ; f_y) \quad (5.6)$$

where C_1, C_2, , C_3, C_4 = unknown coefficients of the model that need calibration. The first part of equation 5.2 is similar to the ACI code guideline, but the constant values in the ACI code are assumed to be unknown coefficients in the GA model. The second part of Eq. 5.2 is also similar to the ACI code, but it is assumed in the ACI code that the stress at

failure in the transverse stirrups is always f_y, which is not always a true assumption. Stress can be much lower in transverse stirrups when cracks initiate in fibre-reinforced polymer sheets. For selecting the format of the third part of the object function, different functions were tested. Equation 5.1 was used and ε_{fe} was calculated using equation 2.5. The results show that a power function best describes the effective strain at failure for different kinds of FRP materials and mechanisms of their attachment (Fig. 5.1). Knowing the general form of the predictive equation, the model was optimized using the Genetic Algorithms toolbox in a Matlab environment.

In previous works, calibration of codes is based on Eq. 5.1, where V_f represents the shear capacity which is added to the ultimate shear capacity of a beam without FRP sheet attachments. The strong nonlinear capability of the genetic algorithms approach makes it possible to optimize all factors simultaneously and to consider the interaction of the shear capacity provided by concrete, FRP and/or steel. In the present model, the predictive equation was solved directly by using the ultimate shear capacity in the GA target points.

5.5 Results and Discussion

5.5.1 *Optimization of coefficients C_1 and C_2*

Table 5.2 shows the results for optimizing C_1, which is mostly related to the aggregate interlock effect. Previous works generally suggest a constant value of C_1 for different configurations and material types of FRP laminates used in rehabilitation systems.

However, the present study shows that there is a significant difference between the value of C_1 for different FRP materials and application schemes. Because the failure of the concrete element and the rupture or debonding of the FRP laminates do not occur simultaneously, especially for two or there sided laminate applications, it is likely that FRP laminates will fail well below the point at which concrete reaches its load capacity. After failure of the FRP sheets, all the stress will suddenly be transmitted to the concrete and steel.

Results show that using CFRP in a four-sides bonded scheme leads to better performance, and generally in a completely wrapped scheme, the C_1 coefficient is 16% greater than that for two or three-sides bonded application for carbon fibre-reinforced polymers, and 26% greater for glass fibre-reinforced polymers, respectively. There was not sufficient data available in the open literature on two or three-sides bonded beams with Aramid (Kevlar) FRP RC beams.

Table 5.2 also shows the results for optimizing the C_2 coefficient. This factor mainly shows the effect of longitudinal rebars on the ultimate shear capacity. It can be observed that the C_2 coefficient has a higher value for completely wrapped systems. It can be concluded that the completely wrapped scheme is a better choice not only because FRP sheets will undergo higher strain before failure, but also because other elements (concrete and steel) can reach their maximum capacity before failure.

5.5.2 *Optimization of coefficients C_3 and C_4*

The coefficients C_3 and C_4 relate to the final strain level in the FRP sheets ε_{fe} and are shown in Table 2. It can be observed that generally, in the completely wrapped scheme, the strain level in the FRP laminate will generally be closer to the ultimate strain than that for two- or three-sides bonded application, and that CFRP provides better results because it has the highest C_3, and the lowest C_4 coefficients compared to that of GFRP and AFRP. This means that it is more likely that CFRP sheets reach its maximum capacity than in the case of other FRPs.

The performance of the proposed genetic algorithm-based equations and that provided by other existing models was investigated using the testing experimental database described earlier, based on both the ratio of the experimental to the corresponding calculated shear strength (V_{exp}/V_{cal}), and the average absolute error (AAE) calculated using Eq. (5.7)

$$AAE = \frac{1}{n}\sum \frac{\left|V_{\exp} - V_{cal}\right|}{V_{cal}} \times 100 \tag{5.7}$$

The average, standard deviation (SD), and coefficient of variation (COV) for V_{exp}/V_{cal} and AAE for all shear design models investigated are listed in Table 5.3. Figure 5.2 shows the bar chart of the error associated with each code or model.

5.5.3 *Performance of ACI 440, CSA 860 and ISIS equations*

The ACI 440 code does not consider the interaction between the shear capacity contributed by the concrete, steel and FRP sheets. It does not also consider the effect of the shear span-to-depth ratio on the effective strain level in the FRP sheets at failure. Moreover, the second modification factor K_2 (in Eq. 2.9), sometimes becomes negative, especially for two sided laminated applications, which does not have any physical significance. The ACI 440 model has often underestimated shear capacity results with an average $V_{\text{experimental}}/V_{\text{predicted}}$ ratio of 1.62, and a coefficient of variation of 33%, which is considerably high. The CSA and ISIS codes use the same methodology as ACI guidelines and do not consider the effect of the shear span-to-depth ratio, *a/d*, on the effective strain of FRP sheets at failure. They also underestimated the ultimate shear capacity of FRP-bonded reinforced concrete beams with an average $V_{\text{experimental}}/V_{\text{predicted}}$ ratio of 1.56 and 1.43, respectively, which is also too high.

5.5.4 *Performance of EC2 model*

The EC2 model does neither consider the effect of the shear span-to-depth ratio, *a/d*, on the effective strain of FRP sheets at failure, nor the interaction between concrete, steel and FRP sheets. The EC2 model has often overestimated results with an average $V_{\text{experimental}}/V_{\text{predicted}}$ ratio of 0.91, and a coefficient of variation of 22.4%.

5.5.5 *Performance of Matthys model*

The Matthys model does not consider the interactions between concrete, steel and FRP sheets, but takes into account the effect of the shear span-to-depth ratio. The Matthys model generally overestimated the ultimate shear capacity of FRP-bonded concrete beams with an average $V_{\text{experimental}}/V_{\text{predicted}}$ ratio of 0.94, and a coefficient of variation of 26.2%. This performance is comparable to that the Eurocode EC2.

5.5.6 *Performance of Colotti model*

The Colotti model also does not consider the interactions between the shear capacity contributed by concrete, steel and FRP sheets and ignores the effect of the shear span-to-depth ratio. It uses several formulas to identify the failure type and to predict the ultimate shear capacity of FRP bonded reinforced concrete beams. The Colotti model provides reasonable results with an average $V_{\text{experimental}}/V_{\text{predicted}}$ ratio of 1.08, and coefficient of variation of 18%, yet it needs several parameters that are not always available.

5.5.7 *Performance proposed GA model*

The shear equation optimized using the genetic algorithms approach outperformed other existing design methods and models. It has lower *AAE* (16.5%) and *COV* (15.0%) than that of the other existing models, and estimated the ultimate shear capacity of fibre-reinforced polymer bonded concrete beams more accurately.

5.6 Sensitivity Analysis of Effect of Shear Span-to-Depth Ratio

This study showed that the shear span-to-depth ratio not only affects the shear capacity provided by concrete, but also the shear capacity provided by the steel and external FRP sheets. In this section of this chapter, the effect of the shear span-to-depth ratio was investigated using an example. Figure 5.3 shows the characteristics of the selected retrofitted RC beam. All variables were assumed to be constant except the FRP sheets used to retrofit the beam and the shear span-to-depth ratio of the beam which were variable. To ensure shear failure in all cases, the longitudinal reinforcement ratio was selected to be 0.04, which is relatively high, and a large spacing between stirrups was used (#3 steel stirrups spaced at 150 mm). The nominal compressive strength of the concrete was assumed to be 25 MPa and the specified yield strength of both the transverse and longitudinal steel was assumed to be 460 MPa. Table 5.4 summarizes the selected values for the thickness, Young's modulus along the major axis, and the design rupture strain for the different materials used. This example was solved for both two and three sides bonded (using CFRP or GFRP) beam, and completely wrapped retrofitting schemes (using CFRP or GFRP). The effects of the shear span-to-depth ratio on the shear capacity contributed by concrete, effective strain in the FRP sheets and effective stress in the transverse steel are discussed here.

a) *Shear capacity provided by concrete*

Figure 5.4 shows results for the shear capacity provided by concrete. As expected, increasing the shear span-to-depth ratio slightly decreased the ultimate shear capacity. It

can also be observed that the shear capacity provided by the concrete is not independent of the selection of the FRP type and reinforcement scheme. This interaction effect has been ignored in most previous models. In this example, completely wrapped CFRP sheets showed a better performance, while two or three sides bonded GFRP was less adequate in terms of interaction with concrete.

b) ***Effective strain in FRP sheet***

Figure 5.5 shows the GA model results for the effect of the shear span-to-depth ratio on the effective ultimate strain in FRP sheets. Increasing the shear span-to-depth ratio, *a/d* generally decreases the effective ultimate strain in the FRP sheets. Completely wrapped reinforcement schemes were more likely to experience rupture or to de-bond in stress levels closer to the design ultimate strain.

c) ***Effective stress in transverse steel***

Figure 5.6 shows predicted results for the effect of the shear span-to-depth ratio on the effective stress in the transverse steel. It is shown that the effective stress in the transverse steel can be significantly lower than the yield stress of steel. Previous models generally ignore the interaction effect between concrete, steel and FRP sheets. For instance, the ACI 440 model overestimates the stress level in the transverse steel by assuming that f_y is constant and independent of the shear span-to-depth ratio. Hence, it overestimates the shear capacity provided by the transverse steel and underestimates the shear capacity

provided by the FRP. However, when FRP sheets are about to fail (rupture or de-bonding), it is possible that the stress level in the steel be much lower than f_y. Once the FRP sheets fail, all applied loads have to be carried by the steel and concrete. Thus, the stress level in steel will increase suddenly and overall failure occurs.

5.7 Concluding Remarks

This study proposed shear design equations for RC beams reinforced with externally bonded FRP sheets based on the genetic algorithms method applied to an experimental database of 212 beams collected from the literature. Existing models for this problem are based on regression analysis done separately for the shear capacity contributed by steel, concrete and FRP sheets. Thus, such models are generally unable to consider interaction mechanisms between steel stirrups, concrete and FRP laminates. The following conclusions can be drawn from this work:

(i) The genetic algorithms approach can be used as an effective tool to optimize equations for the shear design of externally bonded FRP reinforced concrete beams. The shear equation optimized using the genetic algorithms approach outperformed other existing design methods and models.

(ii) The stress in steel stirrups at failure can be less than the yield stress, f_y which has not been considered in previous equations and models.

(iii) The ACI 440 method does not consider the effect of the shear span-to-depth ratio on the effective shear strain in FRP laminates, and assumes a linear relationship between the thickness of FRP laminates and the shear capacity contributed by these

FRP laminates, which is not always true. The second modification factor of the ACI code, k_2, sometimes becomes negative, which does not have any physical meaning. This formula often underestimates the shear capacity of FRP retrofitted RC beams.

(iv) The Matthys model considers the effect of the *a/d* ratio on the effective strain of FRP sheets, but is only applicable to CFRP sheets and does not consider the interaction mechanisms between concrete, steel and FRP laminates.

(v) The Colotti model also does not consider the effect of the *a/d* ratio and the interaction mechanisms between concrete, steel and FRP laminates. This model uses several formulas involving parameters that are not always provided in experimental studies, therefore it is not generally simple use.

(vi) It was shown that the completely wrapped scheme provides better results for the shear retrofitting of RC beams compared to other schemes by increasing the confinement of the concrete beam section and consequently the aggregate interlock. On the other hand, the completely wrapped scheme provides better bonding behaviour between concrete and FRP. It was shown that CFRP materials provide better shear capacity in retrofitting RC beams compared to GFRP or AFRP.

(vii) The shear design equations proposed in this study consider both the interaction between concrete, steel stirrups and FRP laminates, and the effect of the shear span-to-depth ratio. Hence, it provided more accurate shear predictions compared to results of the other models considered in this study. RC beams with lower shear span-to-depth ratio are more likely to fail by rupture of FRP sheets. Moreover, concrete and transverse steel rebars in such beams can contribute more shear capacity compared to beams with higher shear span-to-depth ratio.

Table 5.1: Range of design parameters used in experimental database

	a/d	f_c'	b	d	ε_{fu}	r_f	V_n
Minimum	1.1	13.3	64	100	0.0095	0.05	18.75
Maximum	4.0	71.9	600	499	0.0370	12.69	662.00
Average	2.6	39.2	171	254	0.0174	2.16	205.83
***COV* (%)**	25.0	37.0	50	46	39.4	103.2	77.25

Table 5.2: C_1, C_2, C_3 and C_4 coefficients estimated by the GA model

Coefficient	FRP type	Two or three sides bonded	Completely wrapped
C_1	CFRP	0.24	0.28
	GFRP	0.20	0.26
	AFRP	*	0.23
C_2	CFRP	12	14
	GFRP	11	12
	AFRP	*	15
C_3	CFRP	0.23	0.32
	GFRP	0.15	0.27
	AFRP	*	0.15
C_4	CFRP	0.66	0.17
	GFRP	0.92	0.39
	AFRP	*	0.44

* No sufficient data were available for two or three sides AFRP bonded concrete beams in shear testing.

Table 5.3: Performance of shear design equations

Method	*AAE* (%)	*Vexp/Vcal*		
		Average	*SD*	*COV* (%)
ACI-440. 2R-02	59.8	1.62	0.52	33.0
CSA S806-02	52.5	1.56	0.43	27.0
ISIS Canada	46.3	1.43	0.38	27.0
Eurocode (EC2)	27.2	0.91	0.20	22.4
Matthys	29.3	0.94	0.24	26.2
Colotti	22.3	1.08	0.18	17.0
Proposed Equation	16.5	1.00	0.15	15.0

Table 5.4: Properties of FRP sheets selected to investigate the effect of shear span to depth ratio

Material	Thickness t_f, (mm)	Major modulus of elasticity E_f, (MPa)	Design rupture strain, ε_{fu} (mm/mm)
CFRP	0.10	90	0.015
GFRP	0.25	20	0.020

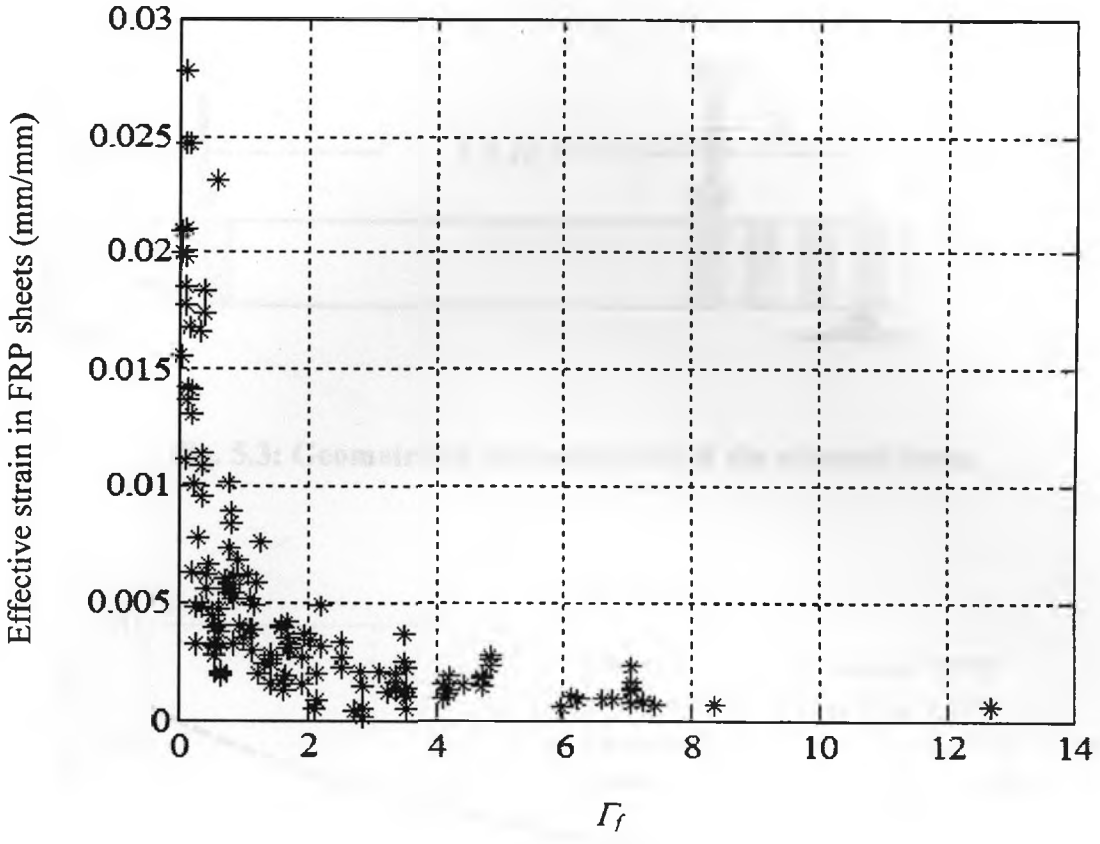

Fig. 5.1: Effective strain in FRP in terms of Γ_f.

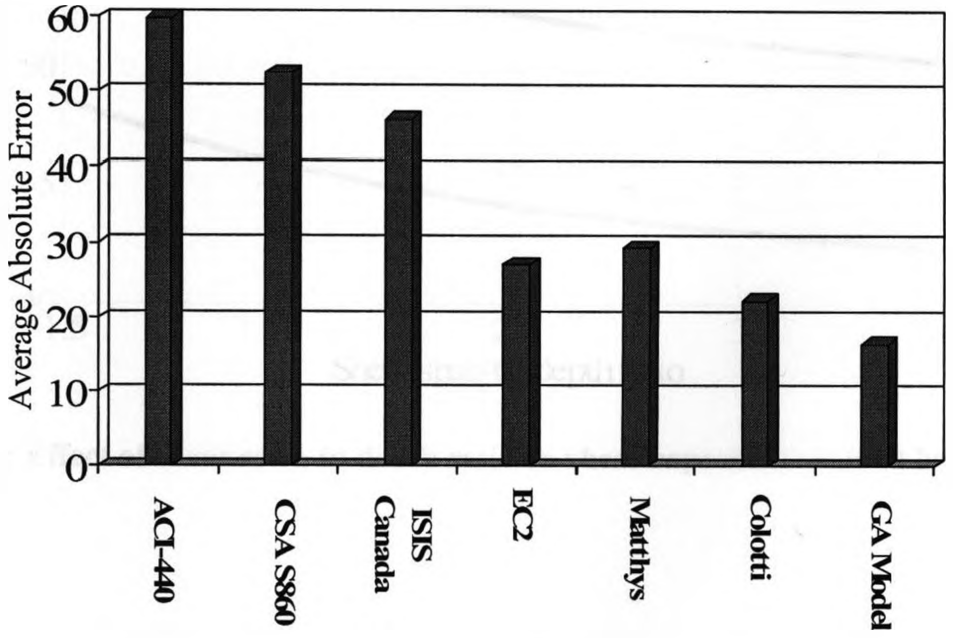

Fig. 5.2: Average Absolute Error (*AAE*) for prediction of shear codes (ACI 440, CSA S860, ISIS Canada and EC2) and models (Matthys, Colotti and GA).

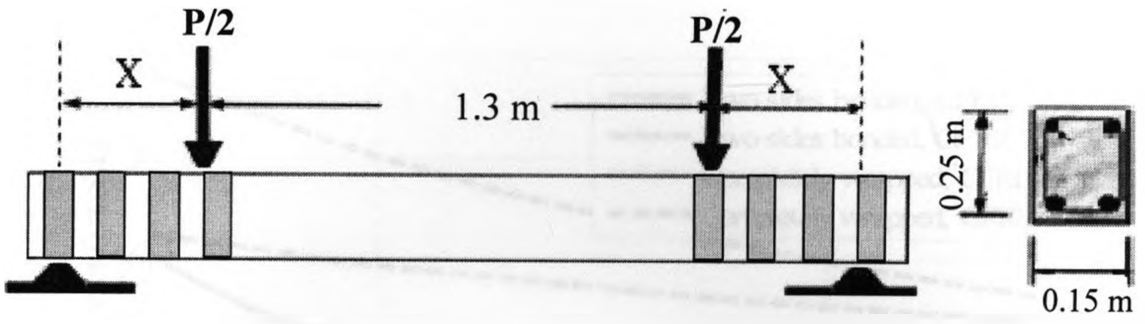

Fig. 5.3: Geometrical characteristics of the selected beam.

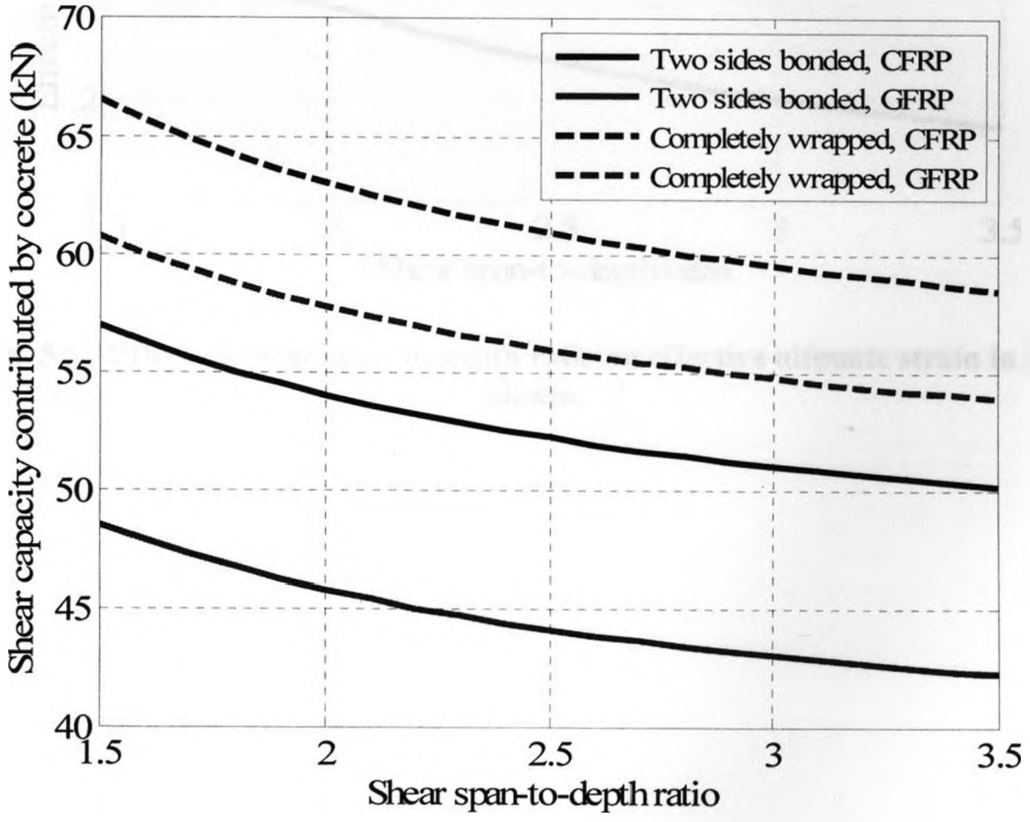

Fig. 5.4: Effect of shear span-to-depth ratio on shear capacity provided by concrete.

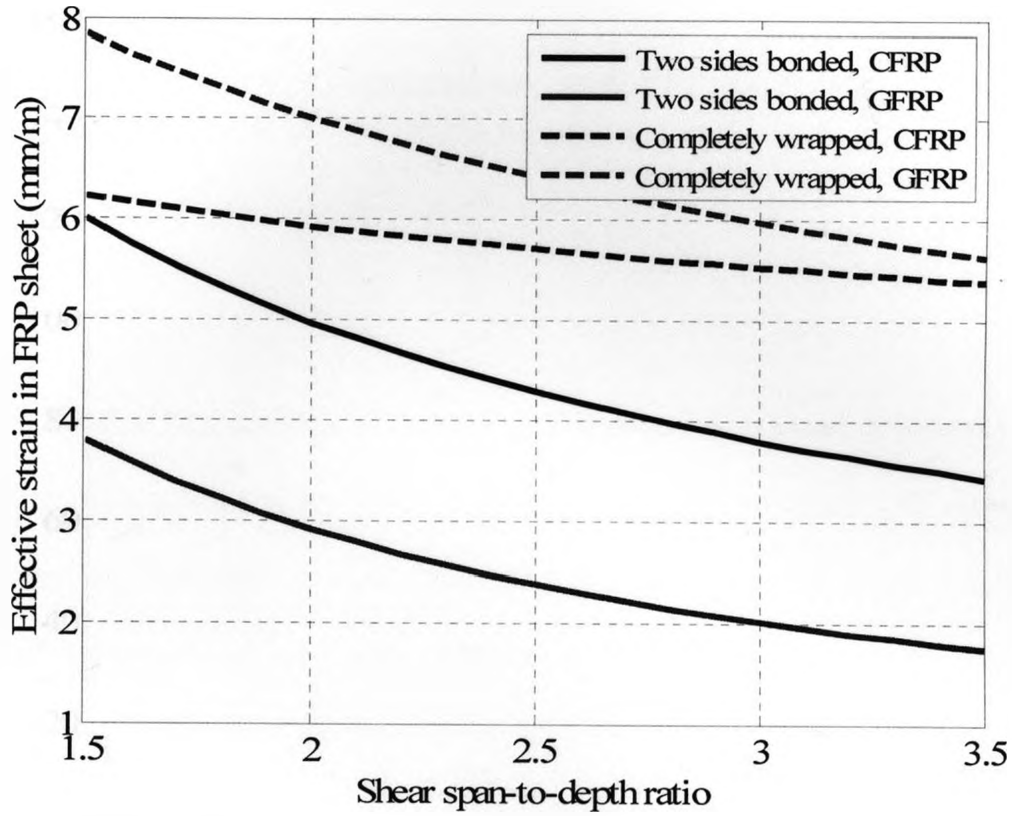

Fig. 5.5: Effect of shear span-to-depth ratio on effective ultimate strain in FRP sheets.

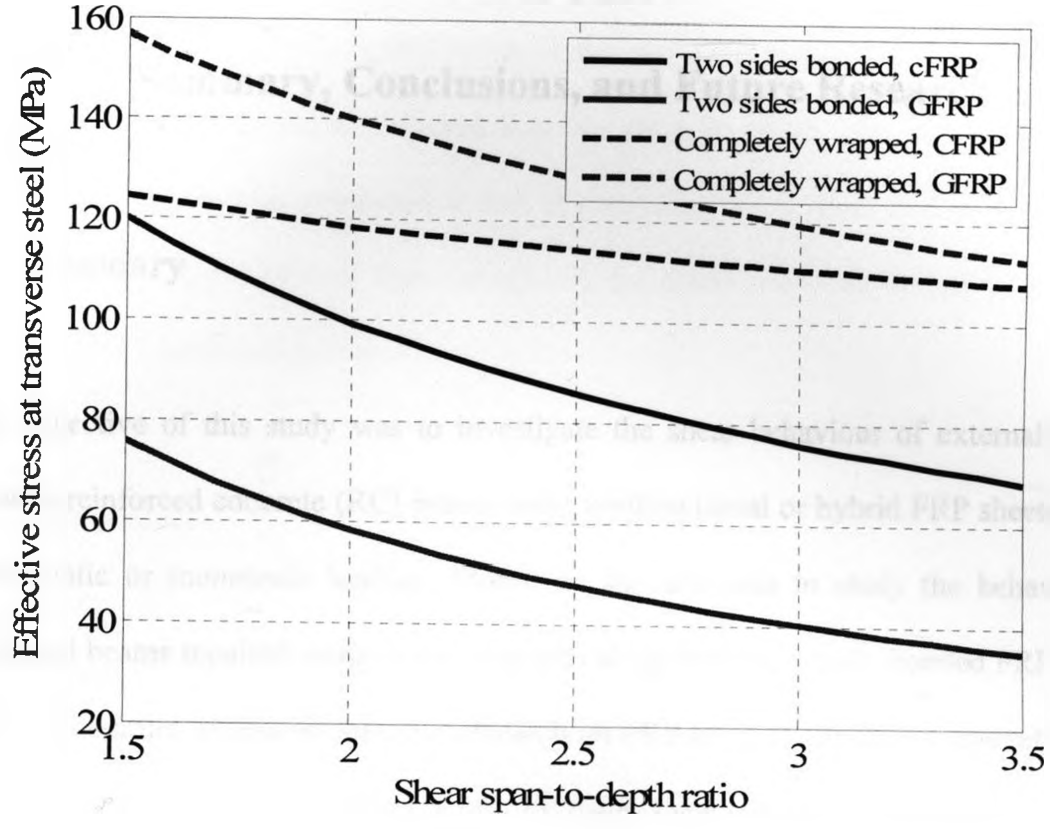

Fig. 5.6: Effect of shear span-to-depth ratio on effective ultimate stress in transverse steel.

CHAPTER 6

Summary, Conclusions, and Future Research

6.1 Summary

The objective of this study was to investigate the shear behaviour of externally FRP-bonded reinforced concrete (RC) beams using unidirectional or hybrid FRP sheets, under quasi-static or monotonic loading. Moreover, the aim was to study the behaviour of damaged beams repaired using epoxy injection along with externally bonded FRP sheets. First, a literature review on previous research on FRP-bonded reinforced concrete beams and current models for predicting the ultimate shear capacity of such beams was conducted. The experimental investigation carried out in this study included the ultimate load capacity, deflection, crack pattern and mode of failure of FRP-bonded reinforced concrete beams. In the fist phase of the experimental study, hybrid and unidirectional fibres were used to retrofit beams. These beams were tested using quasi-static loading. The experimental results of this phase of research were predicted using a numerical modeled based on the Finite Elements Method (FEM) developed in this thesis. In the second phase of the experimental work, cracks in the damaged RC beams were repaired using the epoxy injection method. Unidirectional CFRP sheets were also used to cover the shear span of three of the beams in different schemes. The effect of different parameters such as the retrofitting protocol, shear span-to-depth ratio and application scheme of FRP on shear behaviour of externally FRP-bonded reinforced concrete beams

were investigated. New equations were proposed to calculate the shear capacity of FRP bonded-reinforced concrete beams based on the genetic algorithms approach applied to 212 experimental data points collected from the open literature. The performance of the proposed equations was compared to that of commonly used shear design methods and models namely the ACI 440, Eurocode (EC2), the Matthys Model, Colotti model, CSA and the ISIS Canada guidelines.

6.2 Conclusions

FRP sheets have a great potential for retrofitting concrete structures. The main advantages of FRP sheets are their ease of application and ability to mitigate corrosion problems while having a high strength-to-weight ratio. Research on the application of externally bonded unidirectional FRP sheets for reinforced concrete (RC) beams under monotonic loading is well established, and several analytical and empirical models are available for predicting the ultimate shear capacity of such beams. However, these models generally do not consider the interaction between the internal shear reinforcement and the shear capacity imparted by the FRP. Moreover, these models are generally not applicable for hybrid or bidirectional applications of FRP sheets.

Epoxy injection was found to be a powerful and simple method for repairing cracks in damaged concrete structural members compared to conventional methods such as stitching, drilling and plugging, and routing and sealing. Data on the simultaneous application of epoxy injection and externally bonded FRP sheets is scarce.

The present experimental study showed that hybrid FRP sheets have a better performance in increasing the ultimate shear capacity of RC beams compared with that of unidirectional carbon fibre-retrofitted beam specimens. The co-existence of other fibres like glass or aramid in the transverse direction allow carbon fibres in the main direction to get closer to their ultimate strain capacity by increasing the confinement of FRP laminates and postponing the development of cracks in the concrete surface. RC beams with thicker and stronger FRP sheets are less likely to undergo failure by rupture of the FRP sheet. The FEM model developed in this study gave predictions that confirm with the results above.

Fatigue and repetitive loading affect the ultimate load capacity of RC beams through the formation of micro-cracks in concrete and weakening of the bonding layer between concrete and the external FRP sheets. This effect needs to be quantified and accounted for in cyclic loading. The failure mode is also dependent on the FRP retrofitting scheme, type, internal steel arrangement, and type and position of the applied load. Although GFRP and CFRP are brittle in nature, increasing the ductility of RC beam specimens can be achieved by proper application and retrofitting scheme using such materials.

Crack injection using low viscosity epoxy provides an increase of stiffness in the linear region of the load-displacement curves of repaired RC beams. Moreover, considerable increase in the ultimate strength of repaired RC beams can be achieved by the simultaneous application of epoxy injection and externally bonded FRP. This is likely due to the stronger bond-line of epoxy to concrete strength compared to the tensile

strength of concrete. Whether to observe ductile or brittle behaviour of RC beams repaired with epoxy injection and external FRP sheets is highly dependent of the scheme and type of the attached FRP laminates.

A set of equations was proposed in this study to predict ultimate shear capacity of externally FRP bonded beams under monotonic loading based of Genetic Algorithms Approach. It was concluded that the genetic algorithms approach can be used as an effective tool to optimize equations for the shear design of externally bonded FRP reinforced concrete beams. The shear equations optimized using the genetic algorithms approach outperformed other existing design methods. Due to the strong nonlinear curve fitting abilities of GAs, the interactions between the shear capacity contribution of concrete, steel and FRP are considered in the proposed equations. It was concluded that the stress at failure in steel stirrups can be less than the yield stress, f_y which has not been considered in previous models. Failure of the concrete element and the rupture or debonding of the FRP laminates may not occur simultaneously, especially for two or there sides laminate applications. Hence, it is likely that FRP laminates will fail well below the point at which concrete reaches its load capacity. After failure of the FRP sheets, all the stress will suddenly be transmitted to the concrete and steel.

It was shown that the completely wrapped scheme provides better results for the shear retrofitting of RC beams compared to other schemes by increasing the confinement of the concrete beam section and consequently the aggregate interlock. On the other hand, the completely wrapped scheme provides better bonding behaviour between the concrete and

FRP. It was shown that CFRP materials provide better shear capacity in retrofitting RC beams compared to GFRP or AFRP.

It was also found that current design codes generally underestimate the ultimate shear capacity of externally FRP bonded RC beams. All of the models investigated in this study except, the Matthys, model ignore the effect of the *a/d*. This study showed that the shear span-to-depth ratio has a considerable effect on the shear capacity contributed by concrete, the effective strain in FRP sheets, and the effective stress in the transverse steel. Generally, beams with a lower shear span-to-depth ratio are more likely to experience a shear failure due to the rupture of the FRP sheets. Moreover, steel stirrups in such beams have higher stress at failure, and are therefore more likely to yield compared to RC beams with a higher shear span-to-depth ratio.

6.3 Proposed Future Research

This study focused on the effect of the main experimental parameters that influence the shear behaviour of FRP bonded-reinforced concrete beams. However, various issues related to this subject need further research as follows:

(i) More experimental data are needed to build a comprehensive database for FRP bonded-reinforced concrete beams under cyclic loading.

(ii) More research is still needed to investigate long-term behaviour of FRP bonded reinforced concrete beams.

(iii) More data is needed on the effect of different external FRP reinforcement scheme in the transverse direction.

(iv) More reliable equations can be proposed based on an extended FEM database including more design parameters.

(v) More innovative techniques should be proposed for bonding FRP to the concrete surface.

(vi) The effect of environmental factors such as temperature, moisture and ions penetrations need to be investigated.

(vii) Data on aramid fibre reinforced polymers (AFRP) bonded RC beams, especially on two or three sides bonded schemes, is very limited. Particularly, more research should be done on the seismic behaviour of beams retrofitted with AFRP sheets since AFRP has a better damping behaviour compared to that of CFRP or GFRP.

(viii) Other artificial intelligence techniques such as neural networks or fuzzy logic methods can be applied to extend the numerical and/or experimental database on experimentally FRP bonded-reinforced concrete beams.

REFRENCES

ABAQUS 6.6 User's Manual, ABAQUS Inc., Providence, RI, USA, 2006.

Abdel-Jaber, M.S., Walker, P.R., Hutchinson, A.R., 2003, Shear Strengthening of Reinforced Concrete Beams Using Different Configurations of Externally Bonded Carbon Fibre Reinforced Plates, Materials and Structures , **36**:291-301.

ACI Committee 224R-80. Control of Cracking in Concrete Structures, American Concrete Institute; 1980, Farmington Hills, MI.

ACI Committee 224.1R-93. Causes, Evaluation, and Repair of Cracks in Concrete Structures, American Concrete Institute, 1993, Farmington Hills, MI.

ACI Committee 318R-05. Code Requirement for Structural Concrete and Commentary, American Concrete Institute; 2005, Farmington Hills, MI.

ACI Committee 440.2R-02. Guide for the Design and Construction of Externally Bonded FRP Systems for Strengthening Concrete Structures, American Concrete Institute; 2002, Farmington Hills, MI.

ACI Committee 546R-96. Concrete Repair Guide, American Concrete Institute; 1996, Farmington Hills, MI.

Akkurt, S., Ozdemir, S., Tayfur, G., Akyol, B., 2003, The Use of GA-ANNs in Modeling of Compressive Strength of Cement Mortar, Cement and Concrete, **33**:973-979.

Al-Gadhib, A.H., 2003, Repair and Retrofitting of Deteriorated Reinforced Concrete structures-Three Case Studies, Proceedings of the 6th Saudi Engineering Conference ,Vol. 3, Dhahran:KFUPM:147-56.

Al-Sulaimani, G.J., Sharif, A.M., Basunbul, I.A., Baluch, M.H., Ghaleb, B.N., 1994, Shear Repair for Reinforced Concrete by Fibreglass Plate Bonding, Structural Journal, **91**:458-64

Altin, S., Anil, O., Kara, M., 2005, Improving Shear Capacity of Existing RC Beams Using External Bonding of Steel Plates, Engineering Structures, **27**:781-91.

Araki, N., Matsuzaki, Y., Nakano, K., Kataoka, T., Fukuyama, H., 1997, Shear Capacity of Retrofitted RC Members with Continues Fibre Sheets, Proceedings of the third international symposium on non-metallic (FRP) reinforcement for concrete structures, Japan Concrete Institute, Tokyo, Japan, pp. 515-522.

Bennett, S.C., Johnson, D.J., 1978, Structural Heterogeneity in Carbon Fibers, Proceedings of the fifth London carbon and graphite conference, London, UK, pp.377-86.

Bousselham, A., Chaallal, O., 2006, Shear Behaviour of Reinforced Concrete T-Beams Strengthened in Shear with Carbon Fibre-Reinforced Polymer-An Experimental Study, Structural Journal, **103**: 339-47.

Burgoyne, C., 1999, Advanced Composites in Civil Engineering in Europe, Journal of the International Association for Bridge and Structural Engineering, **9**: 267-73.

Calder, A.J.J., Thompson D.M., 1998, Repair of Cracked Reinforced Concrete: Assessment of Corrosion Protection, Crowthorne, Berkshire, Bridges Division, Transport and Road Research Laboratory, Research Report 150.

Canadian Standards Association (CSA). 2002, Design and Construction of Building Components with Fibre-Reinforced Polymers, Canadian Standards S806-02, Rexdale, Ontario, Canada.

Cao, A.Y., Chen, J.F., Teng, J.G., Hao, Z., Chen, J., 2005, Debonding in RC Beams Shear Strengthened with Complete FRP Wrap, Composites for Construction, **9**: 417-428.

Carolin, A., Taljesten, B., 2005, Experimental Study of Strengthening for Increased Shear Bearing Capacity, Composites for Construction, **9**:488-496.

Carolin, A., Taljesten, B., 2005, Theoretical Study of Strengthening for Increased Shear Bearing Capacity, Composites for Construction, **9**:497-506.

Chajes, M.J., Januszka, T.F., Mertz, D.R., Thomson, T.A., William, J., 1995, Shear Strengthening of Reinforced Concrete Beams Using Externally Applied Composite Fabrics, Structural Journal, **92**:295-302.

Chen, J.F., Teng, J.G., 2003, Shear Capacity of FRP-Strengthened RC beams: FRP debonding, Construction and Building Materials, **17**:27-41.

Colotti, V., Spadea, G., 2001, Shear Strength of RC Beams Strengthened with Bonded Steel or FRP Plates, Structural Engineering, **127**:367-373.

Colotti, V., Spadea, G., Swamy, N., 2005, Analytical Model to Evaluate Failure behaviour of Plated Reinforced Concrete Beams Strengthened for Shear, Structural Journal, **101**:755-65.

Dussek, I., 1987, Strengthening of Bridge Beams and Similar Structures by Means of Epoxy-Resin-Bonded External Reinforcement , Transp. Res. Rec. No. 785, Transp. Res. Board, Washington, D.C., 21-24.

EC2-Eurocode 1. 1992, Design of Concrete Structures, European Committee for Standardization, Lausanne, Switzerland.

Ekenel, M., Myers, J.J., 2007, Durability Performance of RC Beams strengthened with Epoxy Injection and CFRP Fabrics, Construction and Building Materials **21**:1182-87.

Goldberg, D.E., 1989, Genetic Algorithm in search, Optimization, and Machine Learning, Addison-Wesley, Reading, Mass.

Guadagnini, M., Pilakoutas, K., Waldron, P., 2006, Shear Resistance of FRP RC Beams: Experimental Study, Composites for Construction, **10**: 464-473.

Hadi, M.N.S., 2003, Retrofitting of Shear Failed Reinforced Concrete Beams, Composite Structures, **62**:1-6.

Hamoush, S., Ahmad, S.H., 1997, Concrete Crack Repair by Stitches, Materials and Structures, **30**:418-423

Holland, J.H., 1975, Adaptation in Natural and Artificial Systems, University of Michigan Press, Ann Arbor, Mich.

Hull, D., Clyne, T.W, An Introduction to Composite Materials, Cambridge University Press, New York, New York, 1996.

Huthchinson, R.L., Rizkalla, S.H., 1999, Shear Strengthening of AASHTO Bridge Girders Using Carbon Fibre Reinforced Polymer Sheets, Proceedings of the fourth international symposium on fibre reinforced polymer reinforcement for Reinforced concrete structures, ACI Publications SP-188, pp.945-56.

ISIS Canada. 2001, Strengthening Reinforced Concrete Structures with Externally-Bonded Fibre Reinforced Polymers, Design Manual No. 4, Zukewich, J., ed., The Canadian Network of Centers of Excellence on Intelligent Sensing for Innovative Structures, University of Manitoba, Winnipeg, Canada.

Islam, M.R., Mansur, M.A., Maalej, M., 2005, Shear Strengthening of RC Deep Beams Using Externally Bonded FRP Systems , Cement and Concrete Composites, **27**:413-20.

Jankowiak, T., Lodygowski, T., Identification of Parameters of Concrete Damage Plasticity Constitutive Model, Publishing House of Poznan University of Technology, 2005; ISSN 1642-9303.

Kachlakev, D.I., Barnes, W.A.1999, Flexural and Shear Performance of Concrete Beams Strengthened with Fibre Reinforced Polymer Laminates. Proceeding of the fourth international symposium on fibre reinforced polymer reinforcement for reinforced concrete structures, ACI Publications SP-188, pp.959-71.

Kachlakev, D., McCurry, D.D., 2000, Behaviour of Full-Scale Reinforced Concrete Beams Retrofitted for Shear and Flexural with FRP Laminates, Journal of Composites, **31**: 445-52.

Kage, T., Abe, M., Lee, H.S., Tomosawa, F., 1997, Effect of CFRP Sheets on Shear Strengthening of RC Beams Damaged by Corrosion of Stirrup. Non-Metallic (FRP) Reinforcement for Concrete Structures, Proceeding of the third international symposium, Sapporo, Japan, pp.443-50.

Khalifa, A., Tumialan, G., Nanni, A., Belarbi, A., 1999, Shear Strengthening of Continuous Reinforced Carbon Fibre Reinforced Beam Using Externally Bonded Carbon Fibre Polymer sheets, Proceeding of the fourth international symposium on fibre reinforced polymer reinforcement for reinforced concrete structures, ACI Publications SP-188, pp.995-1008.

Khalifa, A., Nanni, A. 2000, Improving Shear Capacity of Existing RC T-Sections Beams Using CFRP Composites, Cement & Concrete Composites, **22**:165-74.

Klaiber, F.W., Dunker, K.F., Wipf, T.J., Sanders, W.W., 1987, Methods of Strengthening Existing Highway Bridges , Nat. Cooperative Hwy. Res. Program Rep. No. 293, Transp. Res. Board, Washington, D.C.

Labossiere, P., 2000, Fibre Reinforced Polymer Strengthening of the Sainte-Emelie-de-l'Energie Bridge: Design, Instrumentation, and Field Testing, Canadian Journal of Civil Engineering, **27**:916-27.

Li, A., Diagana, C., Delmas, Y., 2002, Shear Strengthening Effect by Bonded Composite Fabrics on RC Beams, Journal of Composite, **33**:225-39.

Li, L.J., Guo, Y.C., Liu, F., Bungey, J.H. 2005, Efficiency of Hybrid FRP Sheets in Strengthening Concrete beams, Proceedings of the International Conference on Repair and Renovation of Concrete Structures, 343-350.

Li, J., Samali, B., Ye, L., Bakoss, S., 2002, Behaviour of Concrete Beam-Column Connections Reinforced with Hybrid FRP Sheet, Composite Structures, **57**:357-365.

Lim, C.H, Youn, Y.S., 2004, Genetic Algorithm in Mix Proportioning of High-Strengthened Concrete, Cement and Concrete, **34**: 409-20.

Maalej, M., Leong, K.S., 2005, Effect of Beam Size and FRP Thickness on Interfacial Shear Stress Concentration and Failure Mode of FRP-Strengthened Beams, Composites Science and Technology, **65**:1148-58.

Malek, A.M., Saadatmanesh, H., 1998, Analytical Study of Reinforced Concrete Beams Strengthened with Web-Bonded Fibre Reinforced Plates or Fabric, Structural Journal, **95**: 343-51.

Matthys, A.M.S., 2000, Structural Behaviour and Design of Concrete Members Strengthened with Externally Bonded FRP Reinforcement, PhD dissertation, Department of Structural Engineering, Faculty of Applied Science, Ghent University, Belgium.

Michael, J., Januszka, T.F., Mertz, D.R., Thomson, T.A., Finch, W.W., 1995, Shear Strengthening of Reinforced Concrete Beams Using Externally Applied Composite Fabrics, Structural Journal, **92**:295-303.

Minoru, K., Toshiro, K., Yuichi U., Keitetsu, R. 2001, Evaluation of Bond Properties in Concrete Repair Materials, ASCE Journal of Materials in Civil Engineering, **13**:98-105.

Mitsui, Y., Murakami, K., Takeda, K., Sakai, H., 1998, A Study on Shear Reinforcement of Reinforced Concrete Beams Externally Bonded with Carbon Fibres Sheets, Compos Interface, **5**:285-95.

Monti, G., Liotta, M.A., 2006, Holistic Design of RC Beams and Slabs Strengthened with Externally Bonded FRP Laminates, Cement and Concrete Composites, **28**:832-844.

Monti, G., Liotta, M.A., 2007, Tests and Design Equations for FRP-Strengthening in Shear, Construction and Building Materials, **21**:799-809.

Mosallam, A., Banerjee, S., 2007, Shear Enhancement of Reinforced Concrete Beams Strengthened with FRP Composite Laminate, Composites Journal Part B, **38**:781-793.

Nehdi, M., El Chabib, H., Said, A. 2007, Proposed Shear Design Equations for FRP-Reinforced Concrete Beams Based on Genetic Algorithms Approach, ASCE Journal of Materials in Civil Engineering **19**:1033-42.

Norris, T., Saadatmanesh, H., Ehsani, M.R., 1997, Shear and Flexural Strengthening of R/C Beams with Carbon Fibre Sheets, Structural Engineering, **123**:903-911.

Pellegrino, C., Modena, C., 2006, Fibre-Reinforced Polymer Shear Strengthening of Reinforced Concrete Beams: Experimental Study and Analytical Modeling, Structural Journal, **103**:720-28.

Ramasamy, J.V., Rajasekaran, S., 1996, Artificial Neural Network and Genetic Algorithm for the Design of Industrial Roofs - a Comparison, Composite Structure, **58**:747-55.

Rita, S., Wong, Y., Frank, J. 2003, Toward Shear Modeling of Reinforced Concrete Members with Externally Bonded Fibre-Reinforced Polymer Composites, Structural Journal, **100**: 47-55.

Saenz, L.P. 1964, Discussion of "Equation for the stress–strain curve of concrete" by Desayi P., Krishnan S., ACI Structural Journal, **61**:1229–35.

Sakar, G., Tanarslan, H.M., Alku, O.Z., 2009, An Experimental Study on Shear Strengthening of RC T-Section Beams with CFRP Plates Subjected to Cyclic Load , Concrete Research, **61**:43-55.

Sato, Y., Ueda, T., Kakuta, Y., Tanaka, T.1996, Shear Reinforcing Effect of Carbon Fibre Sheets Attached to Side of Reinforced Concrete Beams. In: El-Badry MM, editor, Advanced Composite materials in Bridges and Structures, pp. 621-7.

Sato, Y., Ueda, T., Kakuta, Y., Ono, S.1997, Ultimate shear capacity of reinforced concrete beams with carbon fibre sheets, Non-Metallic (FRP) Reinforcement for concrete Structures, Proceedings of the Third Symposium, vol. 1, Japan, pp.499-505.

Shah, S.P., Swartz, S.E., and Ouyang, C., Fracture Mechanics of Concrete, John Wiley & Sons, Inc., New York, New York, 1995.

Shash, A.A., 2005, Repair of concrete beams—a Case Study, Construction and Building Materials, **19**:75-79.

Shin, Y.S., Lee, C., 2003, Flexural Behavior of Reinforced Concrete Beams Strengthened with Carbon Fiber-Reinforced Polymer Laminates at Different Levels of Sustaining Load, ACI Structural Journal, **100**:231-39.

Spadea, G., Bencaridino, F., Swamy, R. N., 1998, Structural Behaviour of Composite RC Beams with Externally Bonded CFRP, Composites for Construction, **2**:132-137.

Swamy, R.N., Jones, R., Charif, A.N., 1996, Contribution of Externally Bonded Steel Plate Reinforcement to the Shear Resistance of Concrete Beams, Repair and Strengthening of Concrete Members with Adhesive Bonded Plates, SP-165, R.N., American Concrete Institute, Farmington Hills, Mich., pp.1-24.

Swamy, R.N., Mukhopadhyaya, P., Lynsdale, C.J., 1999, Strengthening for Shear of RC Beams by External Plate Bonding, The Structural Engineer, **77**:19-30.

Taerwe, L., Matthys, S., 2000, Concrete Slabs Reinforced with FRP Grids. II: Punching Resistance, Composites for Construction, **4**:154-61.

Taljsten, B., 2003, Strengthening Concrete Beams for Shear with CFRP Sheets, Construction and Building Materials, **17**:15-26.

Taljsten, B., Elfgren, L., 2000, Strengthening Concrete Beams for Shear Using CFRP-Materials: Evaluation of Different Application Methods, Composite: Part B, **31**:87-96.

Triantafillou, T.C.1998, Shear Strengthening of Reinforced Concrete Beams Using Epoxy-Bonded FRP Composites, Structural Journal, **95**:107-15.

Tsisatas, G., Robinson, J., 1994, Durability Evaluation of Concrete Cracks Repair Systems, Transportation Research Record 1795, Paper No 02-3596:82-87.

Uji, K., 1992, Improving Shear Capacity of Existing Reinforced Concrete Members by Applying Carbon Fibre Sheets, Trans Japan Concrete Institute, **14**:253-66.

Umezu, K. et al., 1997, Shear Behaviour of RC Beams with Aramid Fibre Sheet. Non-Metallic (FRP) Reinforcement for Concrete Structures, Proceeding of the third international symposium, Sapporo, Japan, pp.491-98.

Wu, G., Wu, Z.S., Lu, Z.T., Ando, Y.B., 2008, Structural Performance of Concrete Confined with Hybrid FRP Composites, Reinforced Plastics and Composites, **27**:1323-48.